GEOLOGY AND GEOCHEMISTRY OF MAGNESITE AND CHROMITE DEPOSITS IN THE ULTRAMAFIC ROCKS OF HARMANCIK, BURSA, TURKEY

A Master's Thesis

Presented by

Samuel KEBEDE Mekete

to

the Graduate School of Natural and Applied Sciences

of Middle East Technical University

in partial Fulfillment for the Degree of

MASTER OF SCIENCE

in

GEOLOGICAL ENGINEERING

MIDDLE EAST TECHNICAL UNIVERSITY

ANKARA

January, 1993

Approval of the Graduate School of Natural and Applied Sciences.

Prof. Dr. Alpay ANKARA
Director

I certify that this thesis satisfies all the requirements as a thesis for the degree of Master of Science.

Prof. Dr. Vedat DOYURAN
Chairman of the Department.

We certify that we have read this thesis and in our opinion it is fully adequate, in scope and quality, as a thesis for the degree of Master of Science in Geological Engineering.

Prof. Dr. Ayhan ERLER
Supervisor

Examining Committee in Charge:

Prof. Dr. Ayhan ERLER

Assoc. Prof. Dr. Asuman TÜRKMENOGLU

Assoc. Prof. Dr. Cemal GÖNCÜOGLU

Asst. Prof. Dr. Nilgün GÜLEÇ

Asst. Prof. Dr. Sönmez SAYILI

ABSTRACT

GEOLOGY AND GEOCHEMISTRY OF MAGNESITE AND CHROMITE DEPOSITS IN THE ULTRAMAFIC ROCKS OF HARMANCIK, BURSA, TURKEY

Samuel KEBEDE Mekete
M.S. in Geological Engineering
Supervisor: Prof. Dr. Ayhan ERLER
January, 1993, 113 pages.

This thesis presents the geological and geochemical studies on magnesite and chromite deposits within the ultramafic complex of Harmancik, Bursa, which is a part of large and discontinuous ultramafic belt in northwestern Turkey . The main lithologic units of the study area, from oldest to youngest age, are: Yanikkaş Marble of Jurassic age, Harmancik ultramafic complex of Late Cretaceous age, Gedikler Granodiorite of Paleocene age and Çakmak Formation of Neogene age. Rocks of the ultramafic complex are represented by harzburgite, dunite and serpentinite. Olivines in dunites are forsteritic, and orthopyroxenes in harzburgites are enstatitic in composition. All ultramafic rocks are affected by serpentinization, which involved addition of H_2O and SiO_2 and removal of MgO.

The ultramafic rocks contain cryptocrystalline

magnesite in vein-type and stockwork type deposits. Veins usually follow minor and major fault planes, whereas stockwork deposits are characteristic of strong brecciation in sheared serpentinites. The magnesite is formed by alteration of the ultramafic rocks by fluids containing CO_2 necessary to form serpentine - magnesite assemblages. Minerals in the veins and stockworks include magnesite, dolomite, chalcedony, quartz, talc, and serpentine. The magnesite contains 80.79 to 99.49 mole percent $MgCO_3$ with 0.49 to 18.62 mole percent of $CaCO_3$ and trace amounts of iron and manganese carbonate. Harmancik magnesite deposit is most probably formed by epithermal solutions. Chromites of the study area are of podiform - type, with the composition of aluminian chromites.

Key Words: Harmancik, Bursa, Ultramafic rocks, Serpentinization, Magnesite, Chromite.

Science Code: 606.03.01

ÖZ

HARMANCIK ULTRAMAFIK KAYACLARI iCiNDEKi MANYEZiT VE KROMiT YATAKLARININ JEOLOJiSi VE JEOKiMYASI, HARMANCIK, BURSA, TüRKiYE.

Samuel KEBEDE Mekete

Yüksek Lisans Tezi, Jeoloji Mühendisligi Anabilim Dali

Tez Yöneticisi: Prof. Dr. Ayhan ERLER

Ocak, 1993, 113 sayfa

Bu tez kuzeybatı Türkiye'deki yaygin ve süreksiz ultramafik kuşagının bir parçası ölan Harmancik - Bursa'daki ultramafik karmaşıgın içindeki manyezit ve kromit yataklarının jeolojik ve jeokimyasal incelemelerini sunar. Çalişma alanının ana litolojik birimleri, yaşlidan gence dogru: Jura yaşlı Yanikkaş Mermeri, Geç Kretase yaşlı Harmancik Ultramafik Karmaşıgı, Paleosen yaşlı Gedikler Granodiyoriti ve Neojen yaşli Çakmak Formasyonudur. Ultramafik karmaşıgın kayaçları harzburjit, dünit ve serpantinittir. Dünitlerin içindeki olivinler forsteritik, harzburjitlerin içindeki ortopiroksenler enstatitik bileşimlidir. Tüm ultramafik kayaçlar, H_2O ve SiO_2 eklenmesi ve MgO taşınmasını içeren, serpantinleşmeden etkilenmişlerdir.

Ultramafik kayaçlar, damar-tipi ve agsi damarcık

tipi kriptokristalin manyezit yatakları içerirler. Damarlar genellikle küçük ve büyük ölçkli fay düzlemlerini izlerken, agsı damarcik tipi yataklar, makaslanmış serpantinitlerdeki yogun breşleşmeile birlikte bulunurlar. Manyezit, serpantin - manyezit toplulugu oluşması için gerekli CO2'yi içeren akışkanların, ultramafik kayaçları dönüştürmesiyle oluşmuştur. Damarlar ve agsı damarciklardaki mineraller, manyezit, dolomit, kalsedon, kuvars, talk ve serpantindir. Manyezit % 80.79 - 99.49 mol $MgCO_3$ ile % 0.49 - 18.62 mol $CaCO_3$ ve çok az miktarlarda demir ve manganez karbonat içerir. Harmancik manyezit yatakları, büyük olasılıkla epitermal çözeltiler tarafından oluşturulmuştur. Çalişma alanindaki kromitler, podiform türde ve aluminyum kromit bileşmindedir.

Anahtar kelimeler: Harmancik, Bursa, Ultramafik kayaçlar, Serpantinleşme, Manyezit, Kromit.

Bilim kodu: 606.03.01

ACKNOWLEDGMENTS

I am very grateful to my supervisor, Prof. Dr. Ayhan ERLER, for his continuous supervision, critical suggestions and thoughtful criticism of the manuscript.

I would like to express my gratitude to Ethiopian Mineral Resources Development Corporation (EMRDC) for giving me the opportunity for further study. Special gratitude is also given to Ethiopian Institute of Geological Surveys (EIGS) and United Nations Development Program (UNDP) who jointly granted me the necessary funds during my stay and study in Turkey.

I am very thankful to the staff of MADKIM (Maden ve Kimya San. Tic. Ltd. Şti) company for their hospitality and cooperation during fieldwork in Harmancik. I extend my gratitude to Mustafa SAGLAM, Mahmud GüLDOST and their families whose hospitality and cooperation made my field work easier.

At last, but not least, I deeply appreciate the staff of Geological Engineering Department (METU) for their continuous cooperation during my study in the Department.

TABLE OF CONTENTS

LIST OF TABLES

LIST OF FIGURES

CHAPTER I

INTRODUCTION

1.1 Purpose and Scope

This thesis presents the geological and geochemical studies conducted on magnesite and chromite deposits and the host ultramafic rock complex at Harmancik - Bursa, belonging to the northwestern ophiolite belt of Turkey. The study area is part of a large ultramafic massif which lies between Dursunbey-Harmancik-Tavşanli townships. The dominant rocks of the study area are harzburgite, dunite, serpentinite and doleritic dikes. Granodiorite and marble crop out in the western part of the area, and Neogene sediments cover the easternmost part of the ultramafic rocks.

The ultramafic rocks of the area are host rocks for cryptocrystalline magnesite and chromite deposits. Magnesite deposits of vein - type and stockwork - type are economically important. At present, a number of deposits are being mined by a private company, MADKIM (Maden Ve Kimya San. Tic. Ltd. Şti), especially in the Çakmak, Mal Pinar, Alakinik Tepe and Adatepe areas. The study area also contains podiform chromite deposits

within dunites. A private company, Hayri Ögelman Madencilik Şirketi, operates the chromite deposits that are located approximately 5 kilometers to the south of the study area. A government owned company, Etibank, also produces chromite at various locations within the Harmancik ultramafic complex.

The purpose of this work is to evaluate the geology and geochemistry of the ultramafic rocks and magnesite and chromite deposits in them. Special attention is given to the rocks of the ultramafic complex and the relationships between dunite, harzburgite and serpentinites are investigated. The geochemical, mineralogical and petrological relationships of these rocks are also established. These rock units are strongly affected by tectonic activity, and they are not mapped as separate units, but presented as an undifferentiated complex. Nevertheless, rocks that are almost completely serpentinized are mapped as a separated unit. As a rule, the economically viable magnesite deposits occur within such zones and major dislocations.

The cryptocrystalline magnesites of Harmancik area are considered as the most important mineral deposits. The type and nature of the magnesites are investigated. The relationships with host rocks are evaluated on the basis of field observations. Two types of occurrences are known: stockwork-type magnesite

deposits (Çakmak open pit) and vein-type deposits (especially Karakuz and Alakinik Tepe).

Different veins and stockwork type magnesite deposits are compared geochemically in terms of major and minor oxides. Members of the solid solution series of carbonate minerals, namely, magnesite, calcite, siderite and rhodochrosite are considered and mole percentages of these carbonates are determined.

1.2 Methods of Study

Fieldwork in Harmancik area including geological mapping at a scale of 1:25000 (Appendix A.1) and sampling (Appendix A.2) was carried out during the summer of 1991. The geological map prepared by MADKIM was of great help for exactly locating the swarms of magnesite veins of the area. Moreover, information regarding the existing works were obtained by on-site visits and talks with MADKIM's staff.

Mapping involved description of lithologies taking into account the megascopic features and alterations such as serpentinization and carbonate alteration associated with the host rocks. serpentinites are clearly outlined on the basis of features such as brecciations and complete serpentinization which are most conspicuous and characteristic of such zones. Magnesite deposits and chromite lenses are shown on the map. Doleritic dikes are also indicated. Magnesite outlines represent tectonic dislocations and they occur as veins

where there was once a fault.

Three types of samples were collected from the study area. The first group of samples were those of rock units from various ultramafic rocks (harzburgite, dunite, serpentinite), doleritic dikes, marbles, granodiorites and Neogene sediments. A total of 23 rock samples were collected and described in the field and all of them are studied under the microscope. Since there is very little chance of obtaining fresh ultramafic rock sample from the outcrops, some fresh samples were taken for comparison from an underground chromite mine located approximately 5 kilometers to the south of the study area. The group of rock samples collected from the study area are given a prefix R- followed by their sample number (eg. R-37); but rock samples taken from the Hudut underground chromite mine are given a prefix HR- followed by the sample number (eg. HR-3). The second group of samples were those of magnesite ores taken from veins and stockworks. A total of 27 magnesite samples are collected . The samples are given a prefix M to designate that it is magnesite (eg. M-3). Samples are taken both from high grade ores to low grade ores in which sometimes lots of impurities such as host rock enclaves and silica are present. The third group of samples were those from chromite ores. A total of 7 chromite samples were collected. Prefix C- is given to sample number (eg. C-5).

The laboratory study included examination of thin sections and polished sections supplemented by XRD

studies for magnesite, chromite and rock samples. Chemical analyses were also carried out for all groups of samples. AAS and spectrophotometer were employed to determine the chemical constituents of the samples.

1.3 Geographic Setting

The study area is in Southern Marmara Region with elevations between 700 - 1100 m. The Harmancik ultramafic complex lies between the townships of Orhaneli and Harmancik, south of the city of Bursa (Figure 1). Harmancik is approximately 90 kilometers south of Bursa. The study area which lies between Yakuplar village in the northwest and Çakmak village in the northeast (Appendix A.1) is about 14 kilometers northwest of Harmancik, and lies within the coordinates of $29^{\circ}00'44''$ - $29^{\circ}07'30''$ E longitude and $39^{\circ}45'00''$ - $39^{\circ}42'47''$ N latitude.

The topography of the area include rather steeply inclined hills, especially in the western part of the study area, becoming gently inclined to the eastern part. The highest summits are Alakinik Tepe (1011m), Karakuz Tepe (1010m), Çatal Tepe (1110m), Kocaçam Tepe (975m) and Turfal Tepe (910m) (Appendix A.1). The two important perennial streams are Sümbul Deresi and Dervent Deresi (Appendix A.1).

The village and forest roads are of average to good quality, stabilized, and is open to traffic around the year. The areas underlain by the ultramafic complex is highly forested, especially by pine-trees so that most

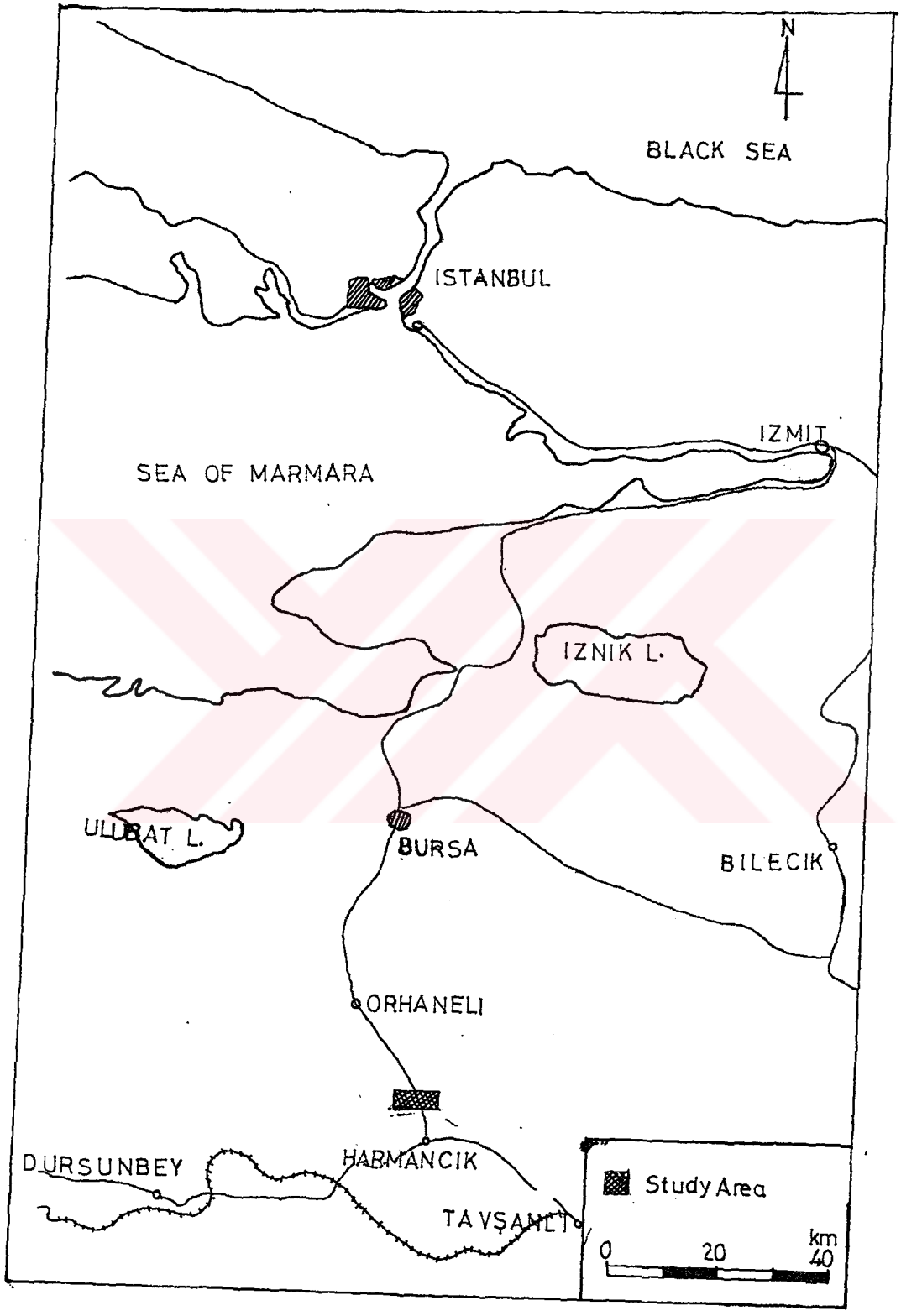

Figure 1 Location Map of the Study Area

of the area is covered by forest. The flat topography together with good development of soil make the granodiorite and the Neogene sediments suitable for agriculture.

1.4 Previous Work

Holzer (1954, in Kalafatçioglu, 1962) studied the geology of the area to the south of Tavşanli and surrounding regions. He proposed the probable age of serpentinite and granites as Late Mesozoic.

Kaaden (1958, in Kalafatçioglu, 1962) studied around the Harmancik region and concluded that the granites are of Late Paleozoic age and the serpentinites are of Early Paleozoic age.

Kalafatçioglu (1962), in his study of the region between Tavşanli and Dagardi mentioned that the ophiolitic sequence was emplaced during the deposition of the sedimentary rocks of the Upper Cretaceous (Maastrichtian) age.

Borchert and Uzkut (1967) studied the regional geological setting of Harmancik ultramafic complex and the surrounding regions and presented a detailed study of chromite deposits of the Harmancik area.

Lisenbee (1971) explained that the Orhaneli ultramafic - gabbro body was emplaced as a thrust sheet in Late Cretaceous; deep faults served as foci for emplacement of granodiorite and dacite intrusions.

Dubertret and Kalafatçioglu (1973) compiled the 1:500000 geological map of Izmir sheet and described the various rock units of the region together with their structural settings.

Tankut (1977) presented a detailed study on the chromites and ultramafic rocks of the Orhaneli massif explaining that the rocks might have originated by differentiation of upper mantle forming a tabular sheet, and the chromites were formed as a direct crystallization from the same source as ultramafics.

CHAPTER II

REGIONAL GEOLOGICAL SETTING

Harmancik region is in northwestern Turkey, very close to the southern edge of the Sakarya zone of Okay (1985) and within the Izmir - Ankara suture zone of Şangar and Yilmaz (1981). The suture zone marks the location of the Tethys ocean and is formed by the collision of the Pontides with the Taurides during Late Cretaceous - Early Tertiary (Şengar and Yilmaz, 1981). The main lithologic units of the region are Paleozoic metamorphics, Mesozoic limestones, Late Cretaceous flysch, Late Cretaceous ultramafics, Early Tertiary granitoids, and Neogene sedimentary and volcanic rocks.

The Harmancik ultramafic complex tectonically overlies a crystalline basement consisting of mica schist, sericitic phyllite, semi marble and calcareous rocks. This unit crops out near Artiranlar village located 8 km away from Harmancik on the Harmancik-Tavşanli road (Borchert, and Uzkut, 1967) (Figure 2.). About 20 km south of the study area, Kalafatçioglu (1962) suggested that the metamorphic rocks are the oldest units (Paleozoic: Dubertret and Kalafatçioglu, 1973) in the region and were affected by the Hercynian Orogeny. Gneisses appear at the lowest part of the metamorphic series, and are overlain by schists

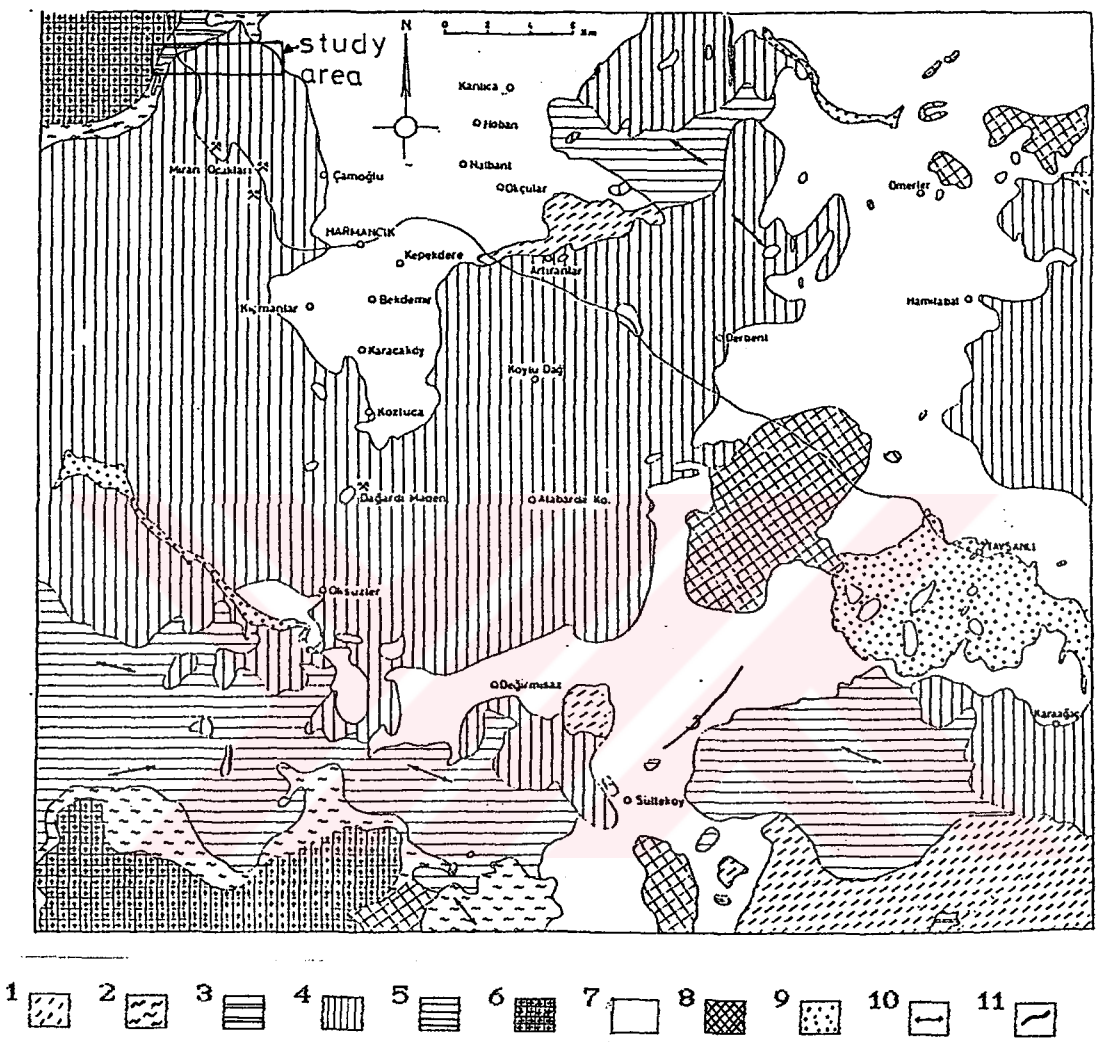

1 2 3 4 5 6 7 8 9 10 11

Figure 3 Regional Geological Map of Harmancik Area.

1- Gneiss - micaschist; 2- Schist; 3- Marble; 4- Ultramafic complex; 5- Limestone and flysch; 6- Granite; 7- Neogene; 8- Volcanics; 9- Alluvium; 10- Fold Axes; 11- Faults (modified from Borchert and Uzkut, 1967).

which occasionally contain lenses and layers of marble. The regionally metamorphosed basement of the Orhaneli area (approximately 30 km north of Harmancik) consists of quartz -mica -schist, marbles, and mafic schists containing glaucophane (Lisenbee, 1971).

At many places, massive to bedded Mesozoic limestones overlie the metamorphic basement. These limestones are of Triassic to Late Cretaceous age (Kalafatçioglu, 1962; Göncüoglu and others, 1992). The limestones are recrystallized to marbles at contacts with granites, this makes the age determination difficult (Borchert and Uzkut, 1967). Marbles of the study area are thrusted over the ultramafic rocks and are intruded by the granodiorites.

During Maastrichtian age, sequences of basalt flows, radiolarian cherts, red limestones, sandstones, and shales were deposited in the Izmir -Ankara zone (Dubertret and Kalafatçioglu, 1973). Kalafatçioglu (1962) mapped these rocks as Upper Cretaceous flysch. The flysch includes allochtonous blocks of serpentinites, volcanic breccias, basalts and limestones (Göncüoglu and others, 1992).

The ultramafic rocks of the study area are part of a large ophiolitic complex which lies between Tavşanli and Dursunbey. Other large ultramafic masses lie at the north in Orhaneli, and at the east in Eskişehir (Figure 3). Lisenbee (1971) suggested that the Orhaneli massif

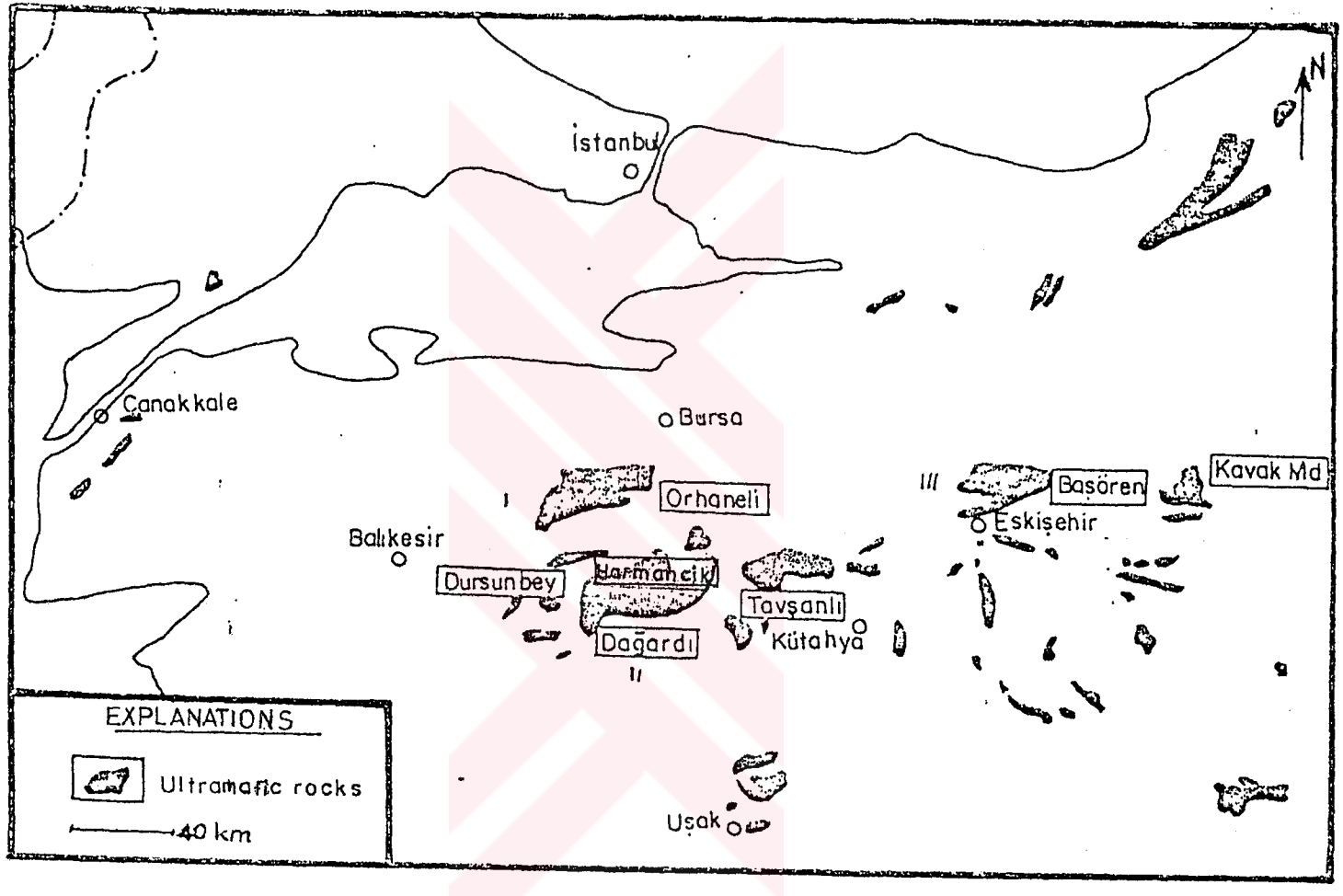

Figure 3- Map showing the locations of the Orhaneli massif and the other ultramafic rocks of Northwestern Anatolia (v.d. Kaaden, 1966, in Tankut, 1977)

might have become detached from these rocks and had moved northward.

The Orhaneli massif in the north is predominantly ultramafic in composition with subordinate clinopyroxenite and gabbro. Ultramafic rocks can be grouped as dunite - clinopyroxenite - chromitite; harzburgite - dunite - chromitite and pyroxenite - gabbro series, with minor hornblendite; chromitite occur exclusively in dunite (Lisenbee, 1971; Tankut, 1977). Within the complex there are numerous fine grained doleritic dikes exposed along shear zones (Tankut, 1977). Lisenbee (1971) mentioned that the dominant structure which characterizes the ultramafic massif is thrust faulting. The faults are defined by bands of serpentine, quartz and chalcedony, and magnesite.

In the previous literature, the age of the ultramafic rocks was regarded to be Paleozoic by Kaaden (1958, in Kalafatçioglu, 1962) and Mesozoic by Holzer (1954, in Kalafatçioglu, 1962: Jurassic - Early Cretaceous) and Kalafatçioglu (1962: Upper Cretaceous). The ophiolitic sequences in the region are accepted to be of Late Cretaceous age (Şengör and Yilmaz, 1981).

Granites occur at the NW and SW corners of the regional geological map (Figure 2). According to Holzer (1954, in Kalafatçioglu, 1962) the outer part of the intrusive consists of light-colored two - mica granite, whereas the central part consists mainly of dark-colored

granodiorite. The granite exposures appear to be fresh with no traces of fracturing, faulting or cataclastic textures (Kalafatçioglu, 1962). The granodiorite pluton intruded the metamorphic basement and the ultramafic complexes of the region. According to Kalafatçioglu (1962) the age of granite is Permian to Triassic, but Holzer (1954, in Tankut, 1977) suggested a Cretaceous-Tertiary age depending on the following evidences: (1) -The granite is surrounded by an older schist with marble blocks in it, (2) -The granite is mostly fresh; no faulting and schistosity are observed, (3) -Maastrichtian limestones in contact with the granite are recrystallized.

A Rb/Sr age determination made on the Büyükorhan pluton (Vachette, 1968, in Lisenbee, 1971) shows an age of 61 $\pm$ 1 Ma (youngest Paleocene), and K/Ar age determination on the Topuk granite (Bingol and others, 1982) indicated an age range of 43 - 63 $\pm$ 3 Ma (Paleocene - Eocene).

After the early phases of the Alpine Orogeny (Late Cretaceous - Early Tertiary) and following uplift, there was a long terrestrial denudation in the area. As a result, Early Tertiary sediments are not observed (Borchert and Uzkut, 1967). During Upper Miocene strong sedimentation occurred in all the freshwater basins of the region. Kalafatçioglu (1962) considered the widespread Neogene (Miocene + Pliocene) sediments in three groups: (1) clastic facies; (2) fresh water facies;

(3) volcanic facies (tuffs and agglomerates). The important volcanic outcrops of the region are found to the east of Tavşanli in a NE - SW direction. Here, andesites, dacites and a small amount of basalt flows are found to be associated with tuffs and agglomerates (Kalafatçioglu, 1962). Miocene starts with a thick conglomerate, containing very large pebbles. Upwards, the conglomerate grades into sands, clays and marls. Above the clays, economically important lignite - bearing sequences are found.

CHAPTER III

GEOLOGY OF THE STUDY AREA

The study area is part of a large ultramafic complex which lies in the northwestern part of Turkey. The dominant rock units are types of ultramafic rocks which are, in order of abundance, harzburgites, serpentinites, dunites and doleritic dikes. This ultramafic complex covers about 85% of the study area, mainly in the central part (Appendix A.1). In the eastern part of the area sedimentary rocks of the Çakmak formation of Neogene age and felsic volcanic rocks overlie the ultramafic rocks (Appendix A.1). Granodiorites and marbles crop out in the western part of the area.

3.1 Yanikkaş Marble

The Yanikkaş Marble crops out between Yakuplar and Gedikler villages (Figure 4). It lies between the Gedikler Granodiorite in the west and the Harmancik ultramafic complex in the east (Appendix A.1). The foliation strikes N20°E and dips 75°NW. The Yanikkaş Marble has granoblastic texture totally composed of recrystallized calcite with graphite along foliation planes (Figure 5). The contact between the marble and the granodiorite is marked by the effect of contact metamorphism induced by the intrusion of granodiorite.

Figure 4. Marble outcrops near Yakuplar.

Figure 5 Photomicrograph of marble, foliated, containing graphite along planes of foliation (sample no. R-21, crossed nicols x40).

Recrystallization of the marble is prominent near the contact and becoming less pronounced outward from the contact. Close to the the boundary with ultramafics, 1-2 cm thick chert bands, parallel to the marble layers are observed. Foliation planes are better developed near this contact than the marble - granodiorite contact. The age of the Yanikkaş Marble is accepted as Jurassic by regional correlation (Kalafatçioglu, 1962; Göncüoglu and others, 1992).

3.2 Harmancik Ultramafic Complex

The dominant rock unit in the study area is the Harmancik Ultramafic Complex which comprises dunites and harzburgites that are serpentinized to various degrees. They cover about 85 percent of the area mapped. Swarms of doleritic dikes are found within the body of the ultramafic rocks. It was not possible to differentiate and set a boundary between dunites and harzburgites. However, serpentinites with intense shearing are mapped separately. A number of magnesite veins and stockwork deposits occur within serpentinites. The highest peaks of the study area (Çatal Tepe, Hazne Tepe, Karakuz Tepe etc) are capped by rocks belonging to the ultramafic complex.

3.2.1 Field Description

Harzburgites, which are the dominant rocks of the area, are distinguished in the field by distinct green to black vitreous pyroxenes, commonly arranged in parallel rows, parallel to the layering, in serpentinized and weathered outcrops. Moreover, harzburgites are coarser

due to the tabular and prismatic pyroxene crystals than the dunites which are fine grained.

Dunite is distinguished in the field, by yellowish serpentinized and locally red brown to orange, sometimes earthy looking, weathered outcrops. Dunites in hand specimen show successive color changes, from the dark olive green of the fresh core through a lighter green or brown to reddish brown zone to the yellowish surface. The dark grey colour of some dunites is found to be due to the released dots of magnetite within the rock, and the reddish colour is due to hematite or limonite associated with probable iddingsite (Tankut, 1977).

Chromite is an abundant accessory of the dunite and disseminated small grains are present in all samples. Locally they may occur as thin layers, only a single grain wide, which pinch out in a few centimeters, or thicken into podiform deposits with widths to five or six meters. Such deposits are unique to the dunitic horizon. The chromite deposits are as a rule surrounded or engulfed by dunitic jackets.

Magnesite occurs in the form of capillary vein fillings and interlacing network which imparts light colours to the otherwise light green rocks. It also gives strength to the otherwise easily weathered rocks of the complex. So one can see bold outcrops of stockwork of magnesite in the ultramafic rocks that can be seen even from large distances.

The doleritic dikes are distinguished in the field by their dark colour, with fine grained, and hard nature. Their dimensions are small and they occupy weak zones.

3.2.2 Petrography

Harzburgite is the main rock unit within the ultramafic complex. Identification or differentiation of harzburgites from dunite and/or serpentinite is somewhat difficult in hand specimen. These rocks usually have gradational contacts. The most common constituents of harzburgites are orthopyroxene (enstatite, bronzite), olivine and subordinate to these are serpentine, carbonates (magnesite + dolomite), opaque minerals (chromite + picotite), and bastite (Figure 6). Most of the sections show cataclastic or crushed texture

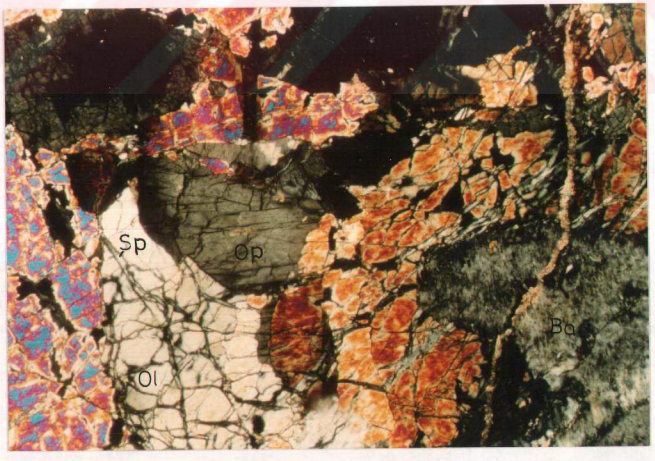

Figure 6. Photomicrograph of harzburgite (sample no. R-29, crossed nicols x 40), Or: orthopyroxene, Ol: olivine, Sp: serpentine, Bas: bastite.

sometimes even appearing as mortar texture.

Olivines are the most strained minerals, and they are usually granulated. They have irregular cracks. These cracks are the sites for the serpentinization process to start. Some of the sections contain serpentine laths, developed in the early stages of serpentinization, arranged in parallel manner (Figure 7).

Orthopyroxenes are determined to be enstatite and/or bronzite by their parallel extinction and absence of pleochroism. They are also distinguished from clinopyroxenes by their low birefringence. Kink banding is characteristic of the orhtopyroxenes. The cleavage traces of orthopyroxenes are generally bent and show wavy extinction, suggesting the activity of deformational forces (Figure 8). Inclusions of olivines in orthopyroxenes form a poikilitic texture.

Disseminations of chromites are common in harzburgites; however, they are less frequent compared to their occurrence in dunites. Sometimes it is possible to see capillaries or trails of chromite in the form of layers. Along with chromite, picotite always occur. The composition of picotite is intermediate between spinel (Mg,Fe), $(Al,Cr)_2O_4$ and chromite $(Fe_2Cr_2O_4)$. The picotite is distinguished from chromite by the yellowish-brown colour, and translucent nature. It is subhedral to euhedral in some samples and anhedral in others (Figure 9).

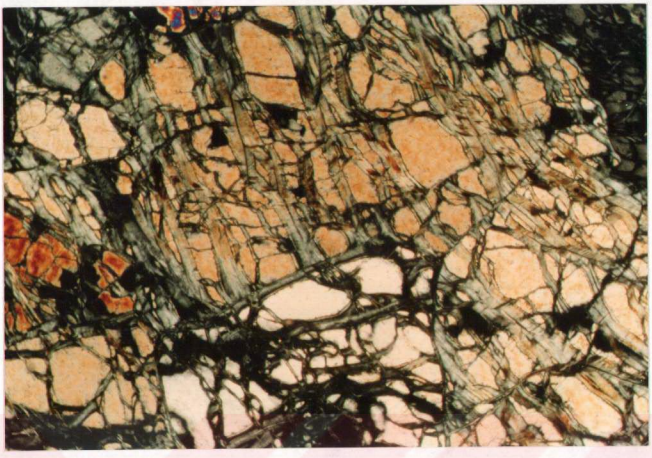

Figure 7 .Photomicrograph of serpentinized harzburgite; serpentines arranged in parallel fashion along crushed grain boundaries (sample no. R-26, crossed nicols x 40).

Figure 8. Photomicrograph of granular orthopyroxene with kink banding shown by bent cleavage trace in harzburgite (sample no. R-4, crossed nicols x40).

Figure 9. Photomicrograph of chromian spinel (picotite) in serpentinized harzburgite; the grains show cataclastic texture (samp. no. R-26, plane light x 40).

Serpentinization is the main alteration process which affects harzburgites of the study area. Both olivine and orthopyroxene are altered to serpentine (the varieties of serpentine are not identified under ordinary petrographic microscope). Mesh-texture is characteristic due to the widespread serpentinization processes resulting in the fibrous network of serpentine in the mass of ultramafic rocks. Occasionally, talc accompanies the serpentine minerals. Capillaries of carbonates are also characteristic, and they might tell us that the solution involved in the alteration process was Mg and Ca carbonate - type water.

Dunite is almost monomineralic and composed of a single olivine phase, however most of the samples from

the study area are enstatite - bearing. The fresh dunite in hand specimen is dark olive green and contains chromite disseminations. The dunite consists of cumulate minerals of coarse anhedral olivine producing a granular interlocking fabric, accessory euhedral to subhedral chromian spinels (chromite and picotite) and orthopyroxene (enstatite) (Figure 10). Kink bands of varied width are common in the olivine. Ubiquitous chromite averages 1 to 2 percent, but greater concentrations are locally present.

The olivine is characterized by the moderate or severe granulation. A common type is enclosure of coarse olivines in a granular matrix of smaller olivines. The lamellar structure of olivines (Figure 11), may be attributed to either the tectonic emplacement or the internal pressure developed during the serpentinization as Engin (1969, in Tankut, 1977) suggested. Wagner and Brown (1968, in Tankut, 1977) suggested for the olivines of stratiform Ruhm intrusion that just after the crystallization and deposition of olivines the weight of the overlying material produced differential stress and consequently strain had developed in olivines.

Ubiquitous chromite is finely disseminated in dunites as an accessory mineral. It is mostly euhedral, but anhedral varieties are not rare. Mostly they are poikilitically enclosed in olivine grains, and also occupy the interstices. Cataclastic deformation is indicated by several irregular fractures, and elongation

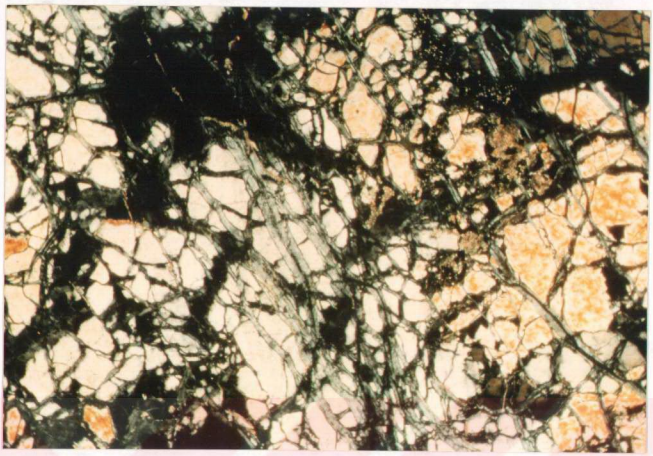

Figure 10. Photomicrograph of serpentinized dunite with crushed olivine grains (sample no. R-3, crossed nicolsx 40).

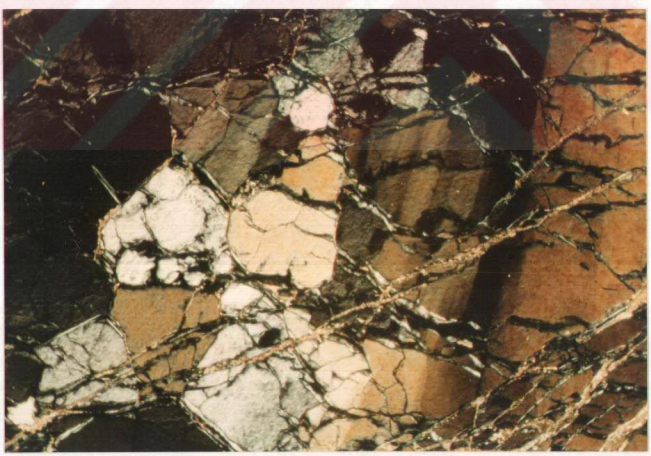

Figure 11. Photomicrograph of strained olivine with wavy extinction, with carbonate veinlets and slight effect of serpentinization (samp. no. R-37, crossed nicols x 40).

of a number of chromite grains, with fractures perpendicular to the elongation (pull-apart texture).

Serpentinization affected the ultramafic rocks to varying degrees. Lisenbee (1971) pointed out that it is related to three causes: 1) faulting, 2) alteration around intrusives, and 3) a paleo-weathering surface. The deep gray-green colour of fresh olivine becomes progressively lighter with increased serpentinization.

Serpentinization occurs throughout the fault zones, increasing in degree toward zones of greater shearing. Quartz, chalcedony and silica-rich magnesite bands are often good indicators of faults, which might otherwise be lost within single units. Serpentinites are also common around doleritic dikes.

Underlying the clastic units of the Çakmak Formation, which cover parts of the ultramafic rocks in the east, is a zone of weathering where dunite and harzburgite were altered to serpentinite; there magnesite veins surrounding blocks of serpentinite may extend downward for tens of meters.

Petrographic study indicates that serpentinites are the major alteration products of ultramafic rocks of the area. They are very common near fault zones and they are usually found bordering magnesite stockworks. Harzburgites and dunites underwent complete serpentinization and become serpentinites in areas of shearing (Figure 12.), and Figure 13 shows relicts of

Figure 12. Photomicrograph of fine grained serpentinite with no traces of primary minerals (samp. no. R-19, crossed nicols x 40).

Figure 13. Photomicrograph of serpentinite with relicts of primary minerals (olivine & orthopyroxene) (samp. no. R-27, crossed nicols x40).

olivines and orthopyroxenes. Degree of serpentinization vary from location to location. It is common to see serpentine with small amount of talc bordering magnesite on both sides of a fault plane. The serpentine is light green in colour, smooth (soapy feeling) with slickensides and striations.

Mesh-structure is typical for serpentinites in which fibrous serpentine minerals form a network. Accessory minerals are primary oxides, chromite and picotite.

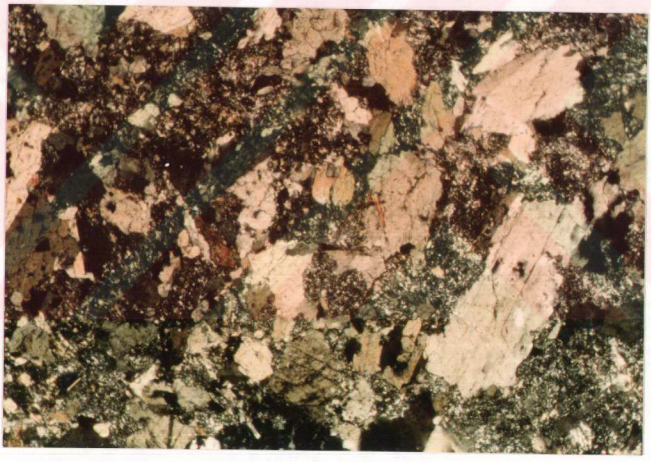

Figure 14. Photomicrograph of dolerite (sample no. R-7, crossed nicols x40).

The dolerite is fine to medium grained, dark coloured and is composed of plagioclase, hornblende, actinolite, chlorite and mylonitized fine grained quartz with small amount of calcite (Figure 14).

3.3 Gedikler Granodiorite

The westmost part of the area, west of Yakuplar and Gedikler villages, is covered by Gedikler Granodiorite which is part of the Buyukorhan pluton. Early in Tertiary time, the metamorphic basement and the Orhaneli ultramafic massif (a little far north of the study area) were intruded by the east-west trending granodiorite Topuk (near Orhaneli) pluton (Lisenbee, 1971). The flat topography together with good development of weathered earth make the granodiorite covered part of the area suitable for agriculture (Figure 15).

Figure 15 Outcrop of Gedikler Granodiorite.

Generally, the Gedikler Granodiorite is a coarse grained, massive and plagioclase rich rock. It has a holocrystalline granular texture composed mainly of plagioclase, quartz, orthoclase, biotite and hornblende.

Almost all the plagioclases show zoning (Figure 16).

A Rb/Sr age determination made on the Buyukorhan pluton by Vachette, et al., (1968, in Lisenbee, 1971) indicated an age of 61 $\pm$ 1 million years (Paleocene).

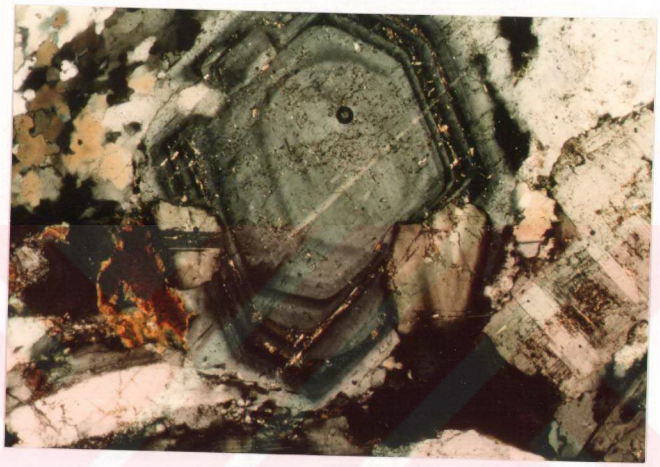

Figure 16. Photomicrograph of Gedikler Granodiorite, plagioclase showing zoning (sample no. R-36, crossed nicols x40).

3.4 Çakmak Formation

The Çakmak Formation crops out in the easternmost corner of the study area. It contains basal conglomerates with immense blocks derived from the ultramafics, dolerites, serpentinites and siliceous rocks. These grade upward to coarse sands (Figure 17) composed of grains derived from a metamorphic terrain, and finally into marls and limestone. Tuffs of intermediate composition are also present (Figure 17). The sedimentary units are part of the Neogene basin that extends from Harmancik to

Figure 17. Sandstone overlain by tuff near Çakmak village.

Orhaneli, which contains some minable coal seams (Borchert and Uzkut, 1967).

The conglomerate is composed of various sizes of rock fragments mainly from the ultramafic rocks cemented by carbonates (Figure 18).

The limestone is typically fine grained, and is composed mainly of calcite and very small amount of clay and opaque mineral (probably magnetite) (Figure 19).

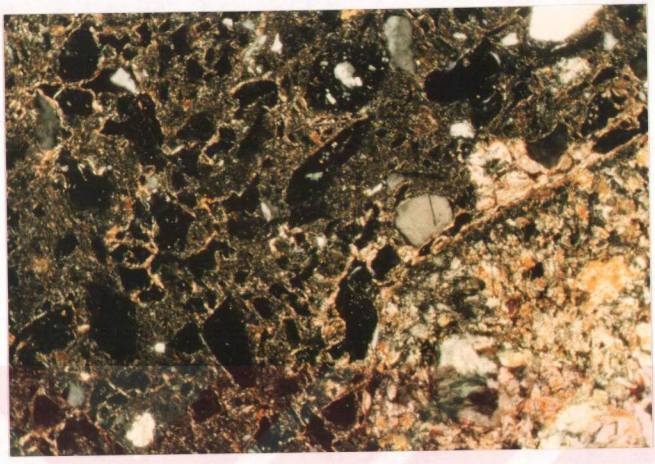

Fig 18. Photomicrograph of conglomerate containing rock fragments derived from ultramafic rocks (sample no. R-13, crossed nicols x40).

Figure 19. Photomicrograph of fine grained limestone (sample no. R-1, crossed nicols x40).

CHAPTER IV

GEOCHEMISTRY OF ULTRAMAFIC ROCKS

4.1 Chemical Composition

Results of chemical analyses of dunite, harzburgite and serpentinite are presented in Table 1. The varied degree of serpentinization of the ultramafic rocks results in varied H_2O (loss on ignition) values and introduces some difficulty in comparing the analyses. So in order to evaluate and compare the analyses, data presented in Table 1. were normalized after subtracting LOI values (Table 2.). This method of presenting the data is suggested by Coleman (1977). The consistency of the $MgO/(MgO + FeO^T)$ value for the dunite and harzburgite as was computed by Coleman (1977) shows us that serpentinization is an isochemical process. Thus, the normalizing process provide a much better comparison between peridotites having varying amounts of serpentinization. The other major chemical variation related to serpentinization is the oxidation of iron, as magnetite is a by-product of this process. For calculation of $MgO/(MgO + FeO^T)$ value in Table 2, total iron is taken as FeO . The values for $MgO/(MgO + FeO^T)$ value for dunites is 0.84 - 0.86 and that for the harzburgite is only slightly lower at 0.82 - 0.85, which are in close agreement with the values of Coleman, 1977,

Table 1. Chemical composition of ultramafic rocks.

oxide wt %	R-29 Harzb.	HR-3 Harzb.	R-37 Dunite	R-3 Dunite	R-25 Serpen.
SiO_2	38.74	37.51	39.1	39.21	39.76
Al_2O_3	0.55	0.34	--	0.23	0.28
Fe_2O_3	2.92	2.48	2.40	2.83	2.78
FeO	5.95	4.56	4.41	5.21	5.15
MgO	39.57	40.36	43.28	41.07	37.75
CaO	0.93	0.34	0.61	0.21	0.07
Na_2O	.001	.03	0.02	.002	.01
K_2O	.04	.02	.02	.02	.05
TiO_2	nd	nd	nd	nd	nd
P_2O_5	.005	--	.023	.015	.003
MnO	.07	.12	.06	.07	.06
NiO	.16	.11	.21	.19	.17
ZnO	.007	.22	.007	.006	.008
Cr_2O_3	.16	.53	.47	.47	--
LOI	9.27	12.29	8.95	10.07	14.11
Total	98.43	98.91	99.56	99.60	100.2

nd- not determined
LOI- loss on ignition

Table 2. Normalized chemical data of the Harmancik ultramafic rocks after subtracting the loss on ignition from the analyses

oxide wt %	R-29 Harzb.	HR-3 Harzb.	R-37 Dunite	R-3 Dunite	R-25 Serpen.
SiO_2	43.45	43.30	43.13	43.79	46.18
Al_2O_3	.61	.39	--	.26	.32
Fe_2O_3	3.27	2.86	2.65	3.16	3.23
FeO	6.67	5.26	4.87	5.82	5.98
MgO	44.38	46.59	47.77	45.87	43.85
CaO	1.04	.39	.67	.23	.08
Na_2O	.001	.03	.02	.002	.01
K_2O	.04	.02	.02	.02	.06
TiO_2	nd	nd	nd	nd	nd
P_2O_5	.006	--	.03	.016	.003
MnO	.08	.14	.07	.08	.07
NiO	.18	.13	.23	.21	.19
ZnO	.008	.25	.008	.007	.01
Cr_2O_3	.18	.61	.52	.52	--
$\frac{MgO}{MgO+FeO^T}$	.82	.85	.86	.84	.83
MgO/SiO_2	1.03	1.08	1.11	1.05	.95

FeO^T-total iron oxide

0.86 for harzburgite and 0.85 for dunite.

Sample R-29, serpentinized harzburgite, and sample R-3, serpentinized dunite have slightly low $MgO/(MgO + FeO^T)$ values than what Coleman (1977) presented for harzburgite and dunite. This tells us the removal of MgO, during serpentinization. However, sample R-37, dunite with little effect of serpentinization and sample HR-3, harzburgite - little affected , have $MgO/(MgO + FeO^T)$ values of 0.86 and 0.85, respectively, and are in agreement with Coleman's (1977) data.

The mean Al_2O_3 content of dunites, from different parts of the world, computed by Coleman (1977) was 0.35% and that of harzburgite was 0.89% Al_2O_3 and the result presented in Table 1 agrees with these averages. The low level of CaO is reflected in the analysed samples and is because of the absence of clinopyroxenes. The phase that may contain CaO is orthopyroxene, in this case.

Na_2O and K_2O are low which is generally in agreement with the reported analyses of peridotites. These results show that the metamorphic peridotites are truly depleted in these elements and the trace amount of alkalies is probably contained within the pyroxenes (Coleman, 1977).

NiO values in the analysed samples have restricted range and these may be attributed to nickel substitution mainly in olivine structure and to a lesser

extent in the orthopyroxene.

The Cr_2O_3 values truly reflect what is contained in the form of opaque chromite disseminations.

Harzburgites and dunites are everywhere serpentinized to variable degrees in the study area. Variability in the result of chemical analyses is due to this serpentinization. Serpentinization involves addition of water and (or) silica to convert dunite or harzburgite to serpentine bearing rock.

Hypothetical reactions representing the most probable chemical changes can be written for serpentinization of peridotites (Coleman, 1977):

$$\underset{\text{olivine}}{2Mg_2SiO_4} + 3H_2O \longrightarrow \underset{\text{serpentine}}{Mg_3Si_2O_5(OH)_4} + \underset{\text{brucite}}{Mg(OH)_2} \qquad (1)$$

$$\underset{\text{olivine}}{2Mg_2SiO_4} + 2H_2O \longrightarrow \underset{\text{serpentine}}{Mg_3Si_2O_5(OH)_4} + \underset{\text{removed}}{MgO} \qquad (2)$$

$$\underset{\text{olivine}}{3Mg_2SiO_4} + 4H_2O + SiO_2 \longrightarrow \underset{\text{serpentine}}{2Mg_3Si_2O_5(OH)_4} \qquad (3)$$

It is not possible to convert olivine to serpentine without addition of silica or subtraction of magnesia, equation (2) and (3), however, if the excess magnesia is used to form brucite, then a dunite can be converted to serpentinite only by addition of water [equation (1)].

If serpentinization of dunite is accomplished only by addition of water , MgO/SiO_2 value should remain

constant. Coleman (1977) pointed out that brucite -bearing massive serpentinites derived from ophiolitic dunites have similar MgO/SiO_2 values (~ 1.23), but the sheared and monomineralic vein serpentinites have MgO/SiO_2 value between 0.99 and 1.00.

R-25 which is serpentinite of the later type without brucite has a MgO/SiO_2 value of 0.95 (see Table 2) close to what Coleman (1977) reported. This indicates that serpentinization in the region involved removal of magnesia and / or addition of silica and water. This holds true for all the analyzed samples and at the same time for the whole of the massif and this supports the possibility of equations (2) and (3).

4.2 XRD study

XRD pattern of the samples were obtained by using JEOL JSDX 100S diffractometer with operating conditions of 40 kv voltage, 30 mA current and Ni - filtered CuKα radiation. Powder samples were filled into a container with a hallow at the center and scanned from 2° to 60° 2θ at a rate of 1° / minute and chart speed of 1cm / minute.

Sample R-37, dunite with little effect of serpentinization process, and HR-3, serpentinized harzburgite were studied by X-ray diffraction method. The X-ray diffraction pattern of R-37 and HR-3 are presented in Figure 20 and Figure 21, respectively.

The diffraction pattern of dunite, indicates the presence of only two phases, olivine and serpentine. Thin section study of this sample indicated little effect of serpentinization. This sample is taken from near the chromitite body located near Hazne Tepe (Appendix A.2). However, the presence of serpentine minerals, ascertained by X-ray diffraction work, shows us there is almost no chance of obtaining fresh ultramafic rock without being serpentinized. By making use of the data from the diffraction pattern of the dunite (R-37), the composition of olivine, which belongs to solid solution series whose end members are forsterite (Mg_2SiO_4) and fayalite (Fe_2SiO_4), is determined. The method involves the calculation of d-spacing of olivine which occur at (130) reflection ($2\theta = 32.2^{\circ}$) and plotting on the diagram given by Yoder and Sahama (1957, in Tankut, 1977) (Figure 22). Based on this procedure, the composition of olivine is found to be 91% forsterite (Fo) and 9% fayalite (Fa). The forsterite composition agrees with the olivine compositional range reported by Tankut (1977) for ultramafic rocks of the Orhaneli massif and also in the compositional range of olivine from other alpine-type peridotites, which, as compiled by Green (1964, in Himmelberg and Coleman, 1968) is typically Fo_{88} to Fo_{93}.

The diffraction tracing of serpentinized harzburgite showed the coexistence of three phases, orthopyroxene (enstatite), olivine and serpentine (antigorite? & chrysotile?). The intensity of

serpentinization is higher for HR-3 than R-37.

The composition of orthopyroxene is determined using the data obtained from the diffraction pattern of HR-3 (Figure 21). The method involves plotting the d-spacings of the reflections $(1\bar{0}31)$ and (060) on the diagram given by Hancok (1964, in Tankut, 1977) (Figure 23). The enstatite composition is found to be 94.4%.

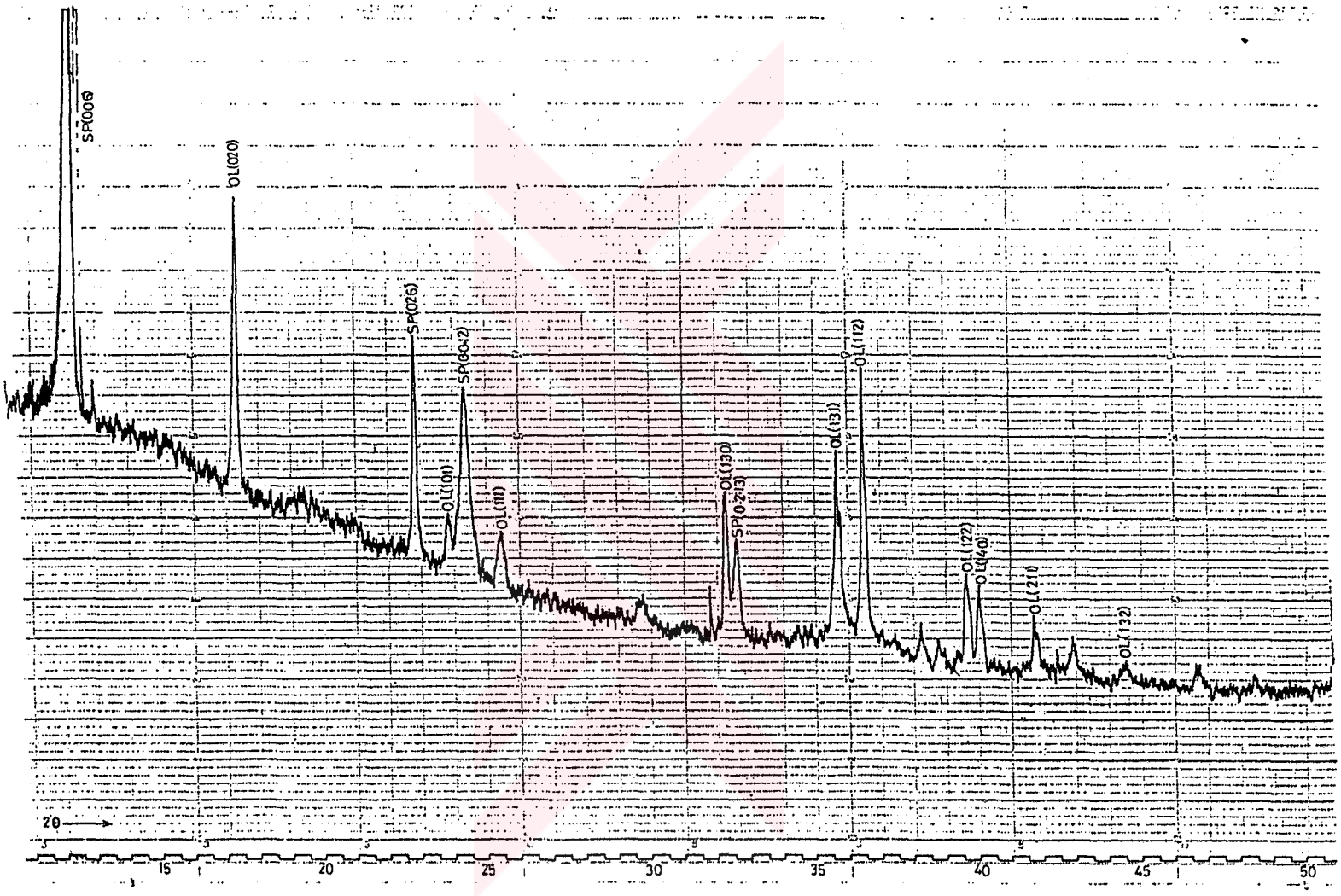

Figure 20 X-ray diffraction pattern of dunite (sample no. R-37). Sp: serpentine; Ol: olivine

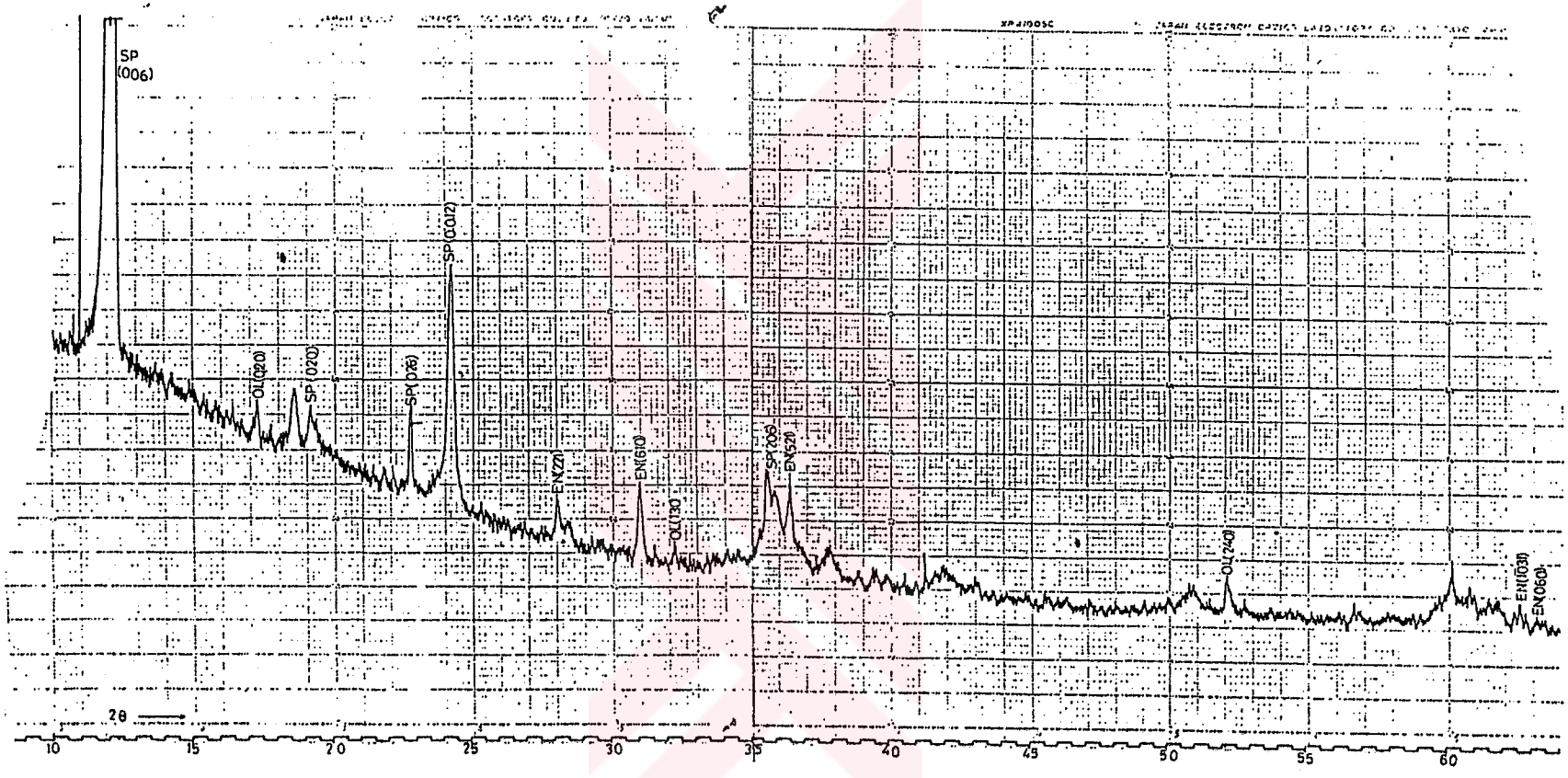

Figure 21 X-ray diffraction pattern of serpentinized harzburgite (sample no. HR-3). SP: serpentine; OL: olivine; En: enstatite

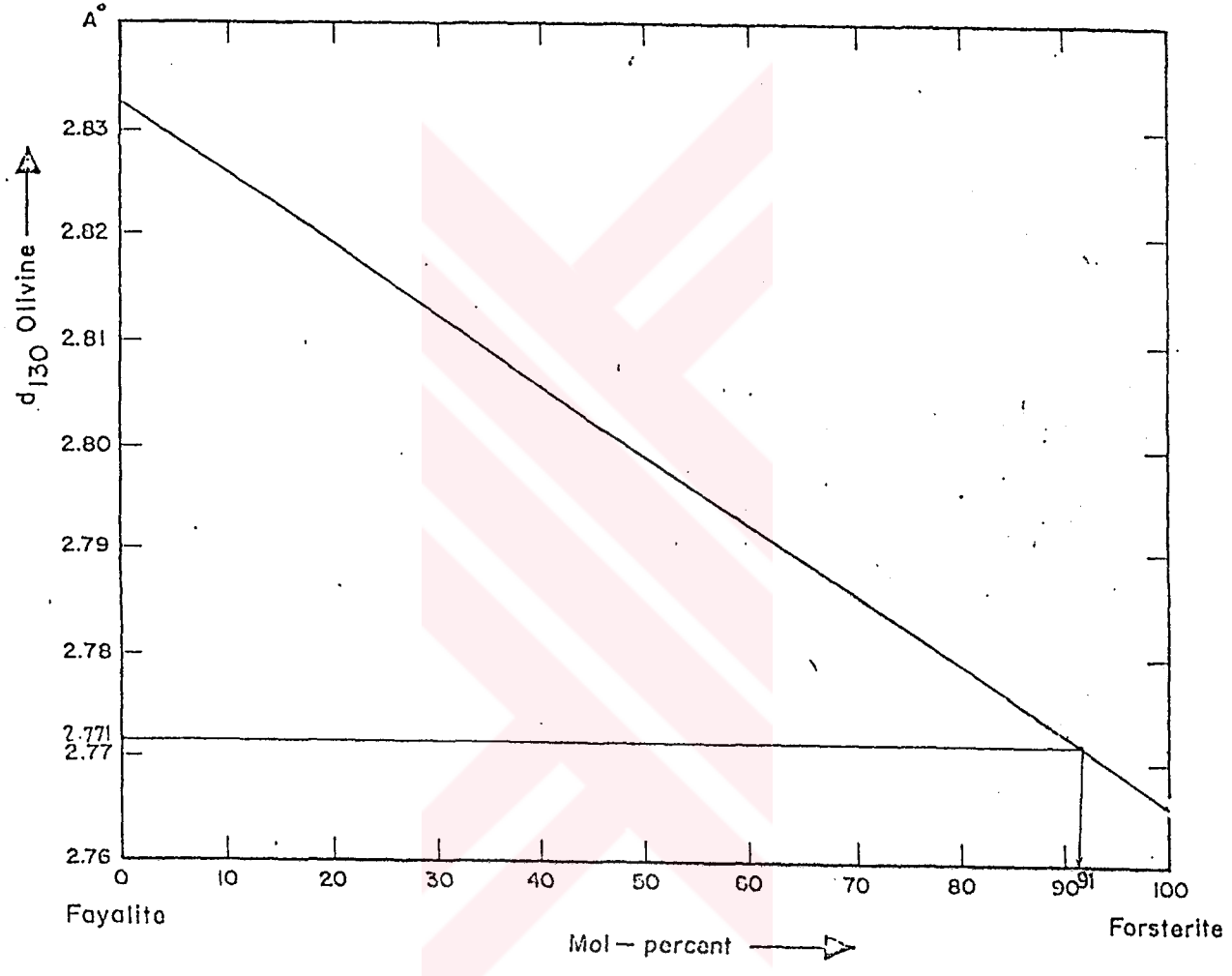

Figure 22 Change of d-spacing of olivine (130) (Yoder and Sahama, 1957, in Tankut, 1977)

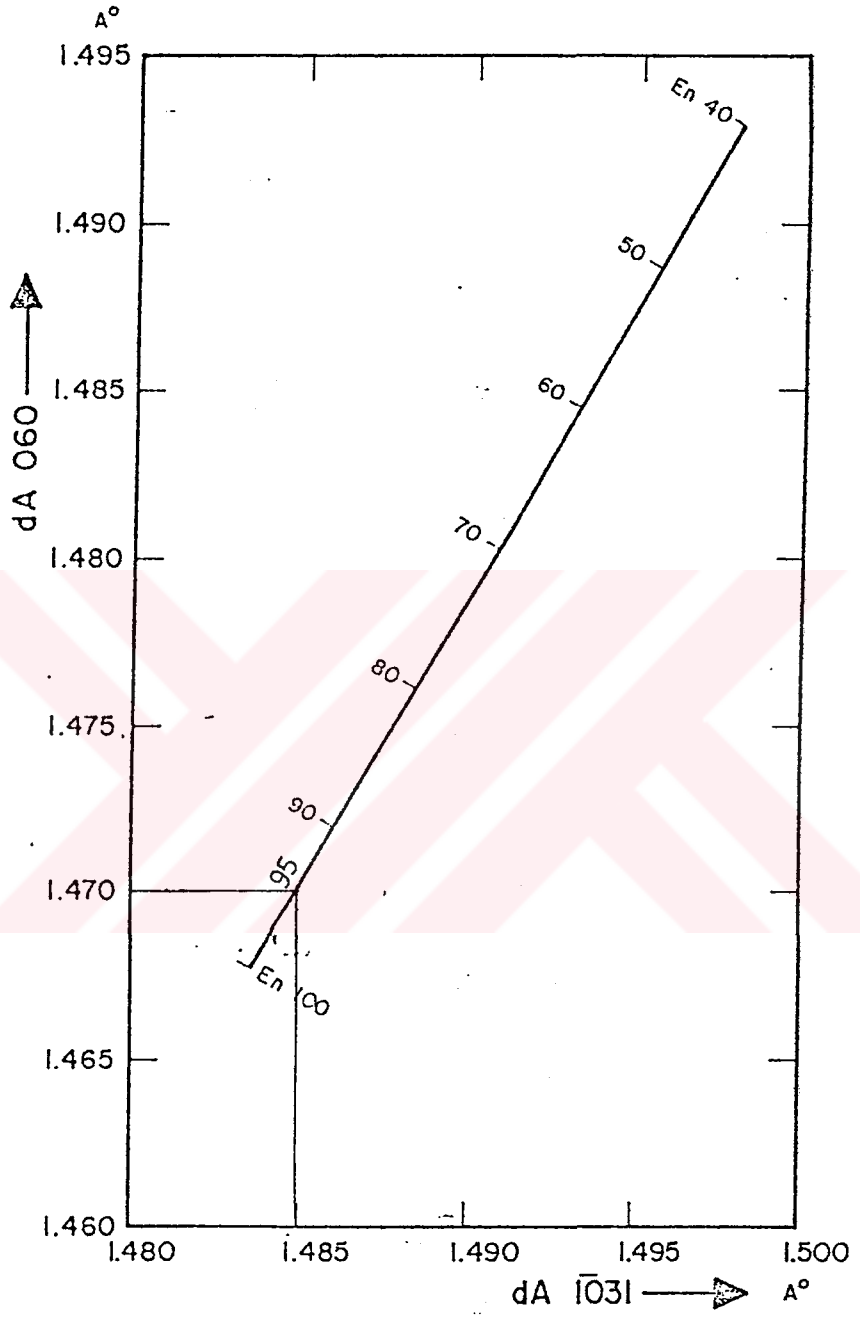

Figure 23. Composition of orthopyroxene by (060) and (1̄031) reflections (Hancock 1964, in Tankut, 1977).

CHAPTER V

MAGNESITE DEPOSITS

5.1 Geological Description

5.1.1 Çakmak Stockwork Deposit (Ia and Ib).

Çakmak deposit is the largest deposit in the study area. It lies on the ridge between Çakmak village in the north and Kocaçam Tepe in the south (Figure 24.). Magnesite has been mined by open pit operations for a long time and the deposit is still promising. According to the mining engineers at the open pit, the present

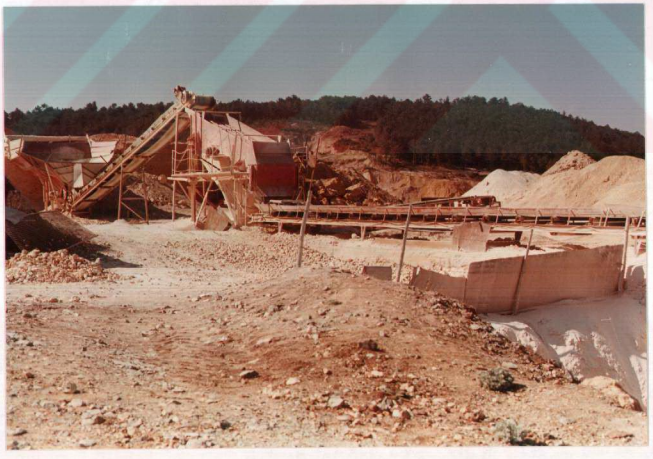

Figure 24. Panoramic view of the Çakmak mine

level of mining is at 80 meters depth from surface. Two types of magnesite are recognized: yellow magnesite (restricted to this deposit) and white magnesite. The yellow color can be attributed to its FeO content. Both cryptocrystalline and crystalline varieties characterize the deposit.

The zone in which the deposit occurs was strongly affected by tectonic activity. It is within the serpentinite of the area. The effects are indicated by the presence of numerous fracture systems in the form of interlacing network along which magnesite veining are conspicuous. The host rock itself which once originally was fresh peridotite was completely serpentinized so that no traces of the original rock fabric are preserved. It is highly weathered, very soft and friable, having a color varying between grey to grayish green.

Within the major stockworks (Figure 25) the effects of repeated deformation are observed and are represented by larger dislocations, along which Mg-Ca carbonates are localized. These strike N 45°E and dip 60° SE. Other numerous veins of magnesite are also found. Their thickness may reach up to 50 cm.

A number of holes were drilled in the Çakmak open pit area. Some of them drilled inside the present limits of the pit, some others to the west and the rest to the north-northwest of it. Some of the drill holes indicate

Figure 25. Magnesite stockwork deposit in Çakmak open pit. The host rock is completely serpentinized ultramafics.

presence of significant magnesite (BATKO Geological Engineering consulting, 1989).

The excavations cover a surface area of 350 meters x 150 meters (52,500 m^2). Snow white magnesite prevails in some parts of the pit (Figure 26.) (position Ia in Appendix A.1) with a north-northwest direction towards the Çakmak village . These occurrences are most likely connected with the magnesite deposits of the pit area (position Ib). Where mineralization in the stockwork is less intense and where the density of veining is low, lenses of the host rock (serpentinite) are still observed. This may indicate that the serpentinite was altered from dunite and/or harzburgite by the same

solutions that deposited the magnesite.

The contacts of magnesite with the host rock is generally irregular for the stockwork in which numerous veinlets of magnesite occur. However, for the larger veins within the stockwork, straight and sharp contacts of magnesite (Figure27) may be the clues for two stages of mineralization.

The magnesite is massive and hard (breaks with a conchoidal fracture). The color ranges from brown-yellowish to snow white. Impurities are generally

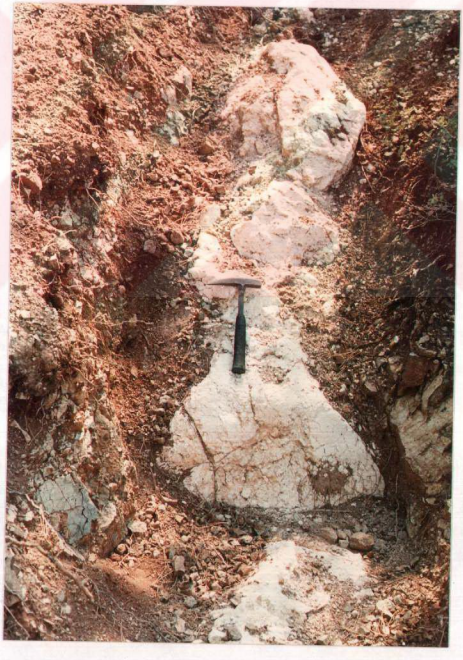

Figure 26. Magnesite vein found in altered ultramafic rock in position Ia of the geological map.

Figure 27. The sharp contact defined by late stage Mg-Ca carbonate fels within the mass of magnesite stockwork.

silica (opal, chalcedony), iron oxides , manganese oxide, and fragments of host rock, serpentinite.

5.1.2 Kocaçam Tepe Stockwork (IIa and IIb)

These stockworks are located very close to Kocaçam T., along the slope to the south of it. Two stockworks are found in the host altered ultramafic rocks with an E-W trend (position IIa). One of them covers an area of 10 x 15m and the other has a width of 15-20m and a length of 140 to 150 meters. The deposit is exposed as a result of small scale mining activity. The magnesite resembles unglazed porcelain and is generally milky white but locally tinted gray, or pink and is hard and massive. Impurities include serpentine, enclosed in or bordering

nodules and associated vein minerals , as well as opal and chalcedony.

5.1.3 Mal Pinar veins (III)

These are four discontinuous veins. They are located 150 meters west of Mal Pinar. Magnesite appears in the form of both vein and stockwork. However, the vein type predominates, unlike the Çakmak deposit. The magnesite is generally snow white, massive, and cryptocrystalline. Along with the major veins, there are a number of small veins. The major vein strikes N 75°E and dips 40° SE; the thickness is up to 0.5 meters. There is also cauliflower type magnesite, which is of good quality.

The boundary is sharp between the magnesite vein and the altered ultramafic rock (Figure 28.). A layer of serpentine containing talc lies between the magnesite and the altered rock. The amount of visible silica in the form of quartz coating vugs and fissures become pronounced near the contact.

This deposit is one of the major deposits of the area. Mining operation still continues and it seems promising for the future.

5.1.4 Başçayir Vein (IV)

This vein is located approximately 500 meters NNW of Başçayir Tepe. The thickness of veinlets is 10-15cm.

The veins are poor in terms of quality, and they contain a lot of host rock enclaves. The general trend of the veins is N60°W dipping gently towards northeast. These veins are found in a topographically flat area and they

Figure 28. Mal Pinar vein-type magnesite deposit showing sharp contact with the host rock.

cover an area of 5 x 40 meters (Figure 29.). Each major vein is surrounded by a stockwork of thinner veins. Locally the host ultramafic rock is lighter in color due to the abundance of carbonate veinlets. The sharp contacts between magnesite and serpentinite are irregular, so complete recovery of the ore is difficult.

5.1.5 Karakuz Tepe Veins (IXa, IXb, IXa)

There are two galleries on the Karakuz Tepe hill. The first one is on the northwest side of the hill, about

900 meters above sea level, with a length of about 130 meters. The width of the magnesite vein is about 2.5 meters. The second gallery on the same vein is at a

Figure 29. Low grade magnesite vein found near Başçayir.

higher elevation with a length of about 37 meters. The width of the vein ranges from 2.5 to 7 meters. At present mining activities in the galleries ceased.

There are swarms of magnesite veins associated with the main vein systems in this part of the region. Although their plan view is discontinuous, most of them might have followed the same fault line. The position IXb on Appendx A.1, for example, shows two magnesite veins localized in the same fault line. This is indicated by the similarity of their attitude, one of which trends

N60°W and dips 60° SW and the other one trends similarly in the direction of N75°W dipping 60°SW (Figure 30). The fault line itself is traversed by late stage faulting which runs in the direction of NE-SW.

The magnesite in hand specimen is rather cryptocrystalline, snow white except light reddish surficial coatings, massive and hard. Crystalline varieties are extremely rare. The host rocks are dunite and harzburgite, serpentinized to various degrees. The degree of silicification is higher close to the contact of the host rock with magnesite veins. Serpentine containing talc is ubiquitous near the contact. However, the degree of serpentinization is less than what is observed in Çakmak stockwork deposit where serpentinization devastates the host rock.

5.1.6 Alakinik Tepe Veins (X)

This vein is located NE of Karakuz Tepe on the Alakinik Tepe. There is a gallery with length of 35 meters. The width of vein is about 2.2 meters. At present mining activity in this gallery given up because of safety conditions. However, by modifying the mining method into an open trench, recovery of magnesite still continues. The trend of the trench strictly follows the strike of the magnesite. The vein strikes N45°W and dips 55°to 65° NE (Figure 31.).

The host rocks are weathered undifferentiated

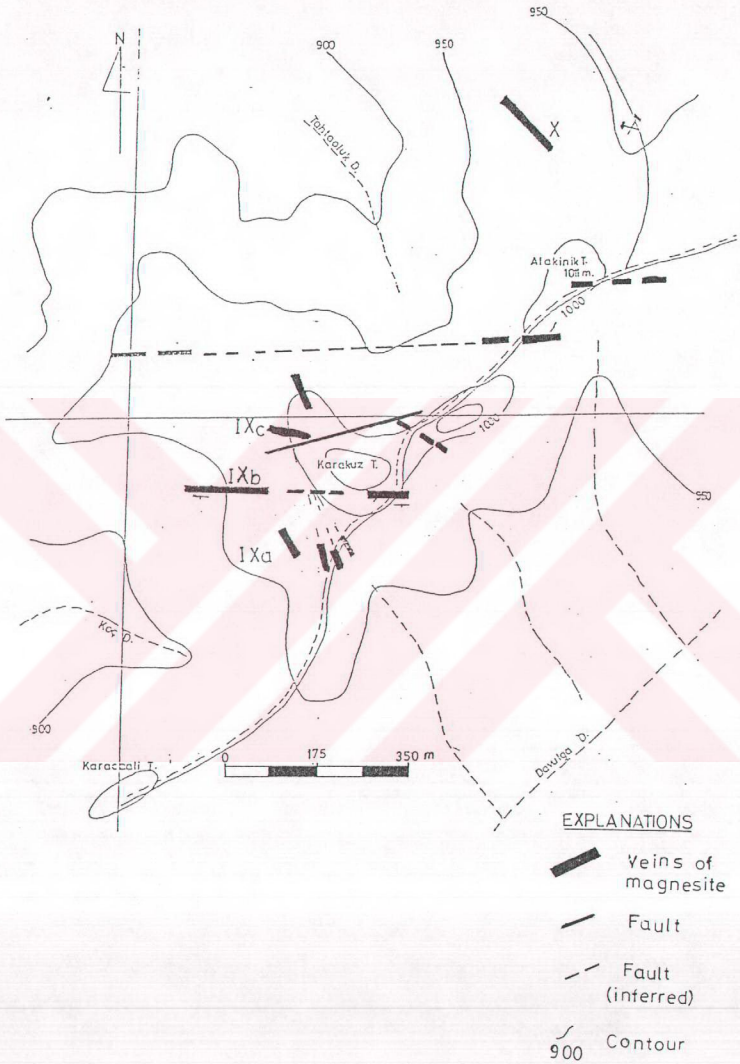

Figure 30. The outcrop map of magnesite veins on Karakuz Tepe and Alakinik Tepe. The possible faults that magnesite veins might have followed are indicated.

ultramafics (dunites and harzburgites), serpentinized to some degree. Alteration becomes pronounced on the contacts with magnesite veins. The concentration of younger doleritic dikes is also higher in this area.

The vein itself occupies a fault line. Fault indicators such as striations and slickensides are clearly observed on the walls of the trench. Smooth

Figure 31. The open pit magnesite mine in Alakinik Tepe. The magnesite follows the reverse fault plane.

surfaces characterize the contact zone especially along with the development of talc bearing serpentinite. Serpentine-carbonate alteration is the major alteration associated with this vein whereas steatitization and silicification are considered as subordinate alteration processes.

The nature of magnesite is not different from that of Karakuz Tepe since they have identical origin and they represent the same episode of mineralization. However, both Karakuz Tepe and Alakinik Tepe veins differ widely from the Çakmak stockwork deposits in that crystalline varieties of magnesite are rare and so far no brownish yellow magnesite, which is characteristic of Çakmak stockwork, is recognized.

5.1.7 Kalempinar Tepe Vein (XI)

This vein is found associated with the chromite pods for which quarry was opened. Having realized the importance of magnesite, the gallery was driven in the direction of N75°W, the trend of the magnesite which dips 60° SW. The vein has a thickness of more than 1m. The magnesite is cryptocrystalline containing quartz filling vugs and cracks.

The host rock is silicified listwaenite containing chalcedony and/or opal with chromite (Figure 32). Serpentinization is pervasive. It is possible to see both chromite and infillings of magnesite within the same mass of the host rock. The contact nature is variable, both sharp and gradational contacts can be observed. The main vein is cut by a number of small veins oriented in several directions.

5.1.8 Adatepe Vein (XII)

This vein is located close to the Adatepe. It is

approximately 50 cm thick and has sharp contacts with the host ultramafic rock. Although it is a little bit far away from the other occurrences, its attitude conforms to the main fissure system of the region. It trends N20°W dipping 40°NE. However, near the contact the ubiquitous

Figure 32. Photomicrograph of listwaenite in which chalcedony form a colloform texture.(samp. no. R-30, crossed nicols x40). An: ankerite, qz: quartz, Sp: serpentine.

association of silica with magnesite, lowers its importance. Due to its small width, the magnesite is not promising for the future. The rock near the contact is altered, but within a few meters, alteration decreases, and fresher specimens can be found (Figure 33.).

5.2 Mineralogy

The best known of the minerals directly and

widely exploited for magnesia content is magnesite, one of the calcite group of rhombohedral carbonates which includes calcite, siderite, and rhodochrosite among others. The members of this group enter into a wide range

Figure 33. Magnesite vein in Adatepe.

of substitutional solid solutions when the positive ions have similar radii. The radii of magnesium and iron ions are within 6% of each other; hence magnesite and siderite form a complete series of which breunnerite (ferroan magnesite) is a well known member. However, the radius of calcium ion is 36% larger than that of magnesium ion, and only limited substitution exists at each end of the magnesite-calcite series.

Magnesite, when pure, contains 47.8% MgO and 52.2% CO_2. The pure mineral is sometimes, but rarely,

found as transparent crystals resembling calcite, but, preponderantly, magnesite may contain considerable amounts of the carbonates, oxides, and silicates of iron, calcium, magnesium, and aluminum. Magnesite may be crystalline or cryptocrystalline. The crystalline form has a hardness of 3.5 to 4.0. The colour may range from white to black with shades of yellow, blue, red, or gray (Birch, and Wicken 1985). The cryptocrystalline (bone magnesite) is massive with no cleavage. The fracture is usually conchoidal, and hardness is 3.5 to 5.0. The color is normally white, but it can have tints of yellow, orange, or buff. Accessory siliceous minerals such as serpentine, quartz, or chalcedony are usually present. Calcium minerals are usually absent or in low concentration in cryptocrystalline magnesite in contrast to their almost invariable presence and higher concentration in the crystalline variety.

Magnesites of the study area are mostly cryptocrystalline, but recrystallized varieties are also found in Çakmak stockwork deposit. The colour varies from white to yellow depending on the presence of impurities.

Petrographic study of magnesite indicated the fine grained nature of magnesite and sometimes the presence of crystalline magnesite (Figure 34 and 35) grains along fractures and zones of strain.

Some of the magnesite samples are studied by

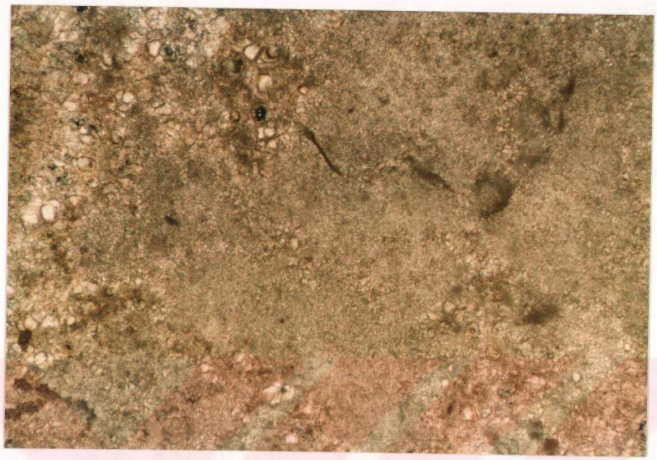

Figure 34. Photomicrograph of recrystallized magnesite in the matrix of fine grained magnesite(sample no. M-3, crossed nicols x40)

Figure 35. Photomicrograph of fine grained magnesite containing talc developed along fractures (sample no. M-4, crossed nicols x40).

X-ray diffraction. The XRD method depicts some of the minerals which could not be possible to determine by thin section study. XRD study was made using JEOL JSDX 100S diffractometer with operating conditions of 40 kv voltage, 30mA current and Ni-filtered CuKα radiation. Powder samples were filled into a container with a hollow at the center (2 x 2 cm and 2mm depth) and scanned from 2° to 60° 2θ at a rate of 1°/minute and chart speed of 1cm/minute. XRD patterns of eight samples were studied (M-6, M-16, M-12, M-8, M-3, M-14, M-13, and M-23) out of which the diffraction patterns of only three samples (M-3, M-6, and M-12) are presented (Figure 36, 37, & 38). The mineral which was not possible to determine by thin section study but determined by XRD method is dolomite. Three samples are found to contain dolomite, namely, M-12, M-8 and M-6 (see Figure 37). These samples especially M-12 and M-8 have appreciable amount of Ca (determined by chemical analyses) which at the same time confirms the presence of dolomite depicted by XRD method. The intensive peaks for both magnesite and dolomite occur at (104) reflection. The coexistence of serpentine with magnesite is indicated by the XRD study of sample M-6 (Figure 38) which represents the equilibrium reaction of Johannes (1969) ($2Mg_2SiO_4 + 2H_2O + CO_2 = Mg_3Si_2O_5(OH)_4 + MgCO_3$).

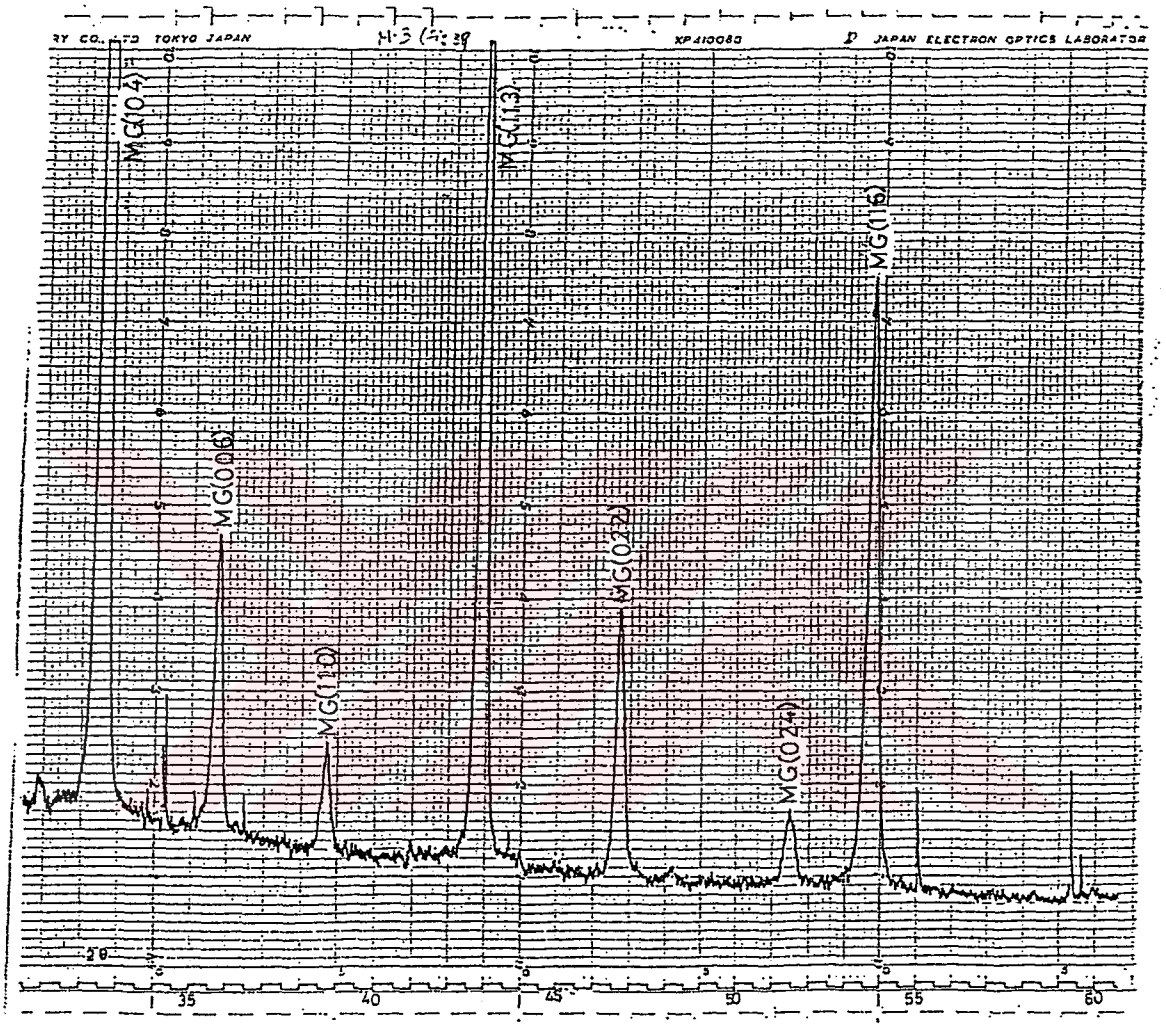

Figure 36 X-ray diffraction pattern of magnesite (Mg) which is almost free from impurities (sample no. M-3).

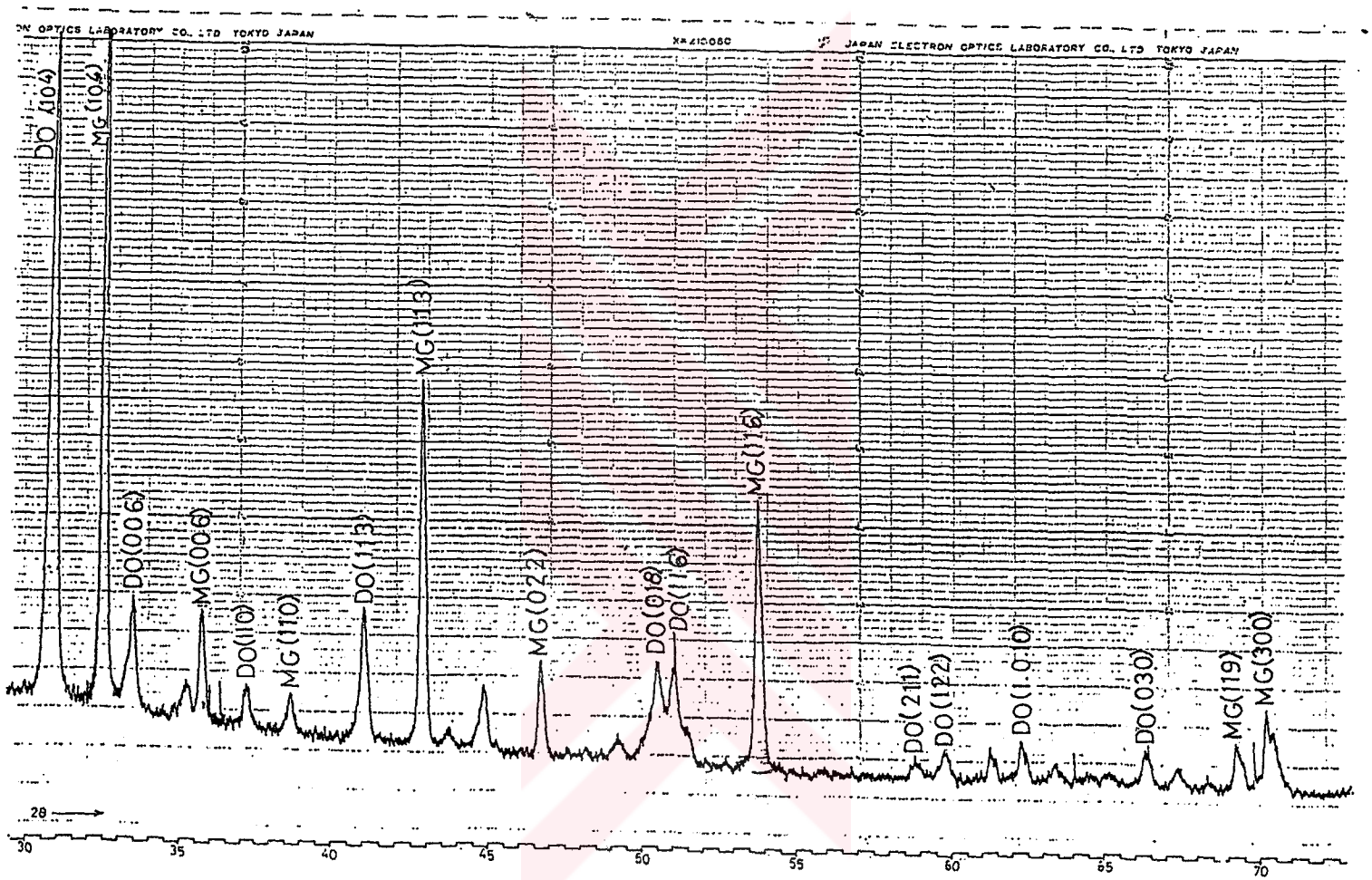

Figure 37 X-ray diffraction pattern of dolomite (DO) bearing magnesite (MG) (sample no. M-12)

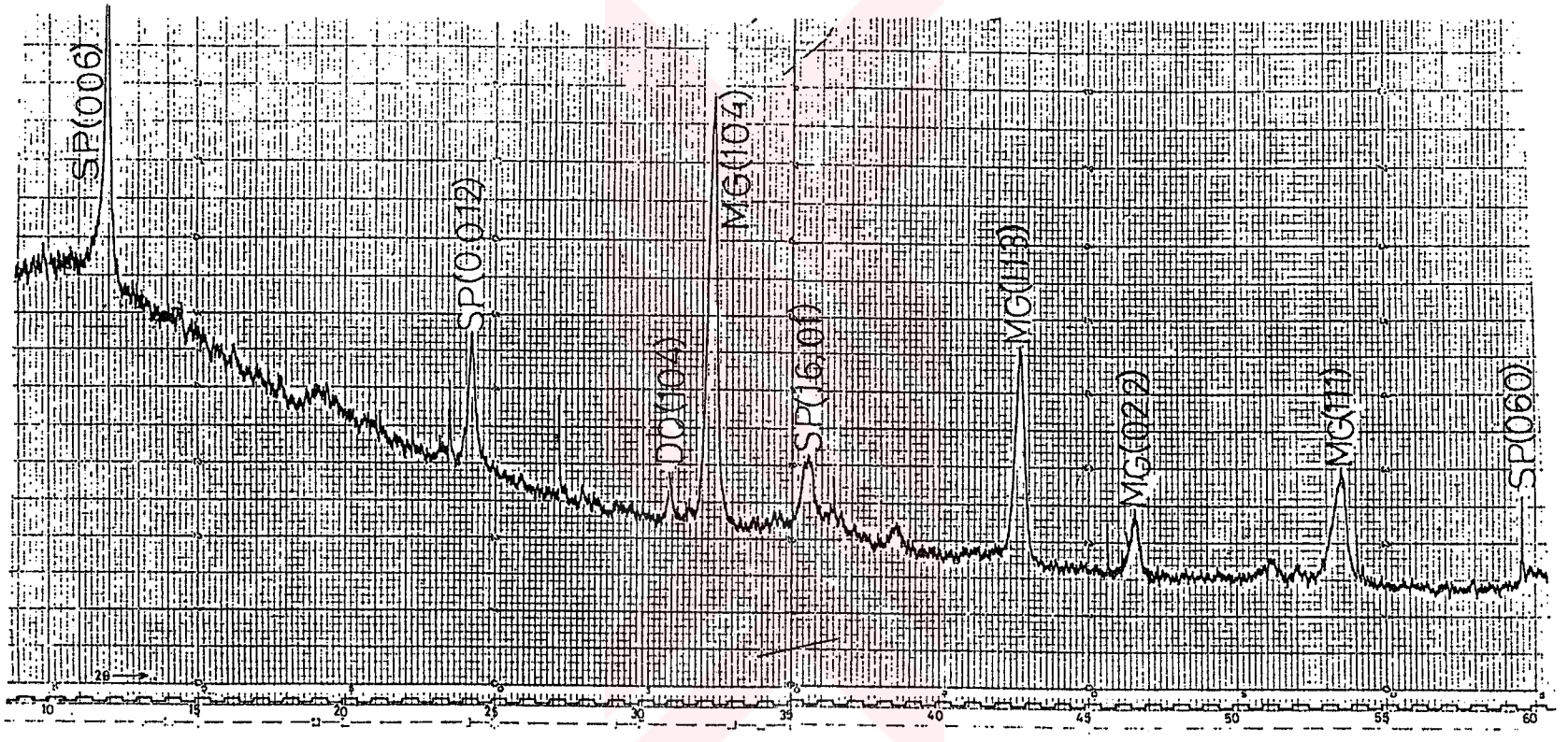

Figure 38 X-ray diffraction pattern of magnesite (MG) containing serpentine (SP) and dolomite (DO) (sample no. M-6)

5.3 Geochemistry

Major and minor elements which are usually or habitually analyzed in magnesites include MgO, CaO, SiO_2, Al_2O_3 and Fe_2O_3 (Pohl, 1990). Analyses of magnesites related with sedimentary units from Czechoslovakian deposits contain a statistically significant body of data (Pohl, 1990). These data show that magnesite contains less silica and alumina than its immediate carbonate country rocks. Trace elements which may substitute in the magnesite lattice are Fe, Cu, Co, Sc, Zn, Ni, Mn, V, Cr, Ti, and B (Möller, 1989). Chemical data on cryptocrystalline magnesite associated with ultramafic rocks reflect little systematic coverage (Zachmann and Johannes, 1989). Industrial standard analyses show that Fe and Ca are commonly lower than those in magnesite of sedimentary origin; SiO_2 contents of run-of mine ore vary considerably. Where Fe is higher, it occurs usually as fine grained hematite giving the magnesite a reddish color and/or contained in the lattice of magnesite. Silica may be due to silicification of magnesite or to free quartz coating vugs and fissures. Trace element contents have been reviewed by Möller (1989); predictably, some elements common in the country rocks (Ni, Co, Cr) may be relatively high although with widely scattering values; their presence in magnesite would probably often be due to trace mineral contents, not to inclusion in the magnesite lattice.

5.3.1 Sample Preparation

Samples of magnesite collected from the ore bodies were first crushed by laboratory scale jaw crusher and then pulverized to -200 mesh size particles using eccentric pulverizer. These powders of magnesite were decomposed by mixtures of acids using the technique of solution B preparation which is described in the Appendix B.1. Silica was determined from solution A using the procedure shown in the appendix B.2.

5.3.2 Analytical Method

The samples were analyzed by making use of atomic absorption spectrophotometer (AAS) and spectrophotometer. Elements analyzed by AAS are: Al, Ti, Fe, Mg, Ca, Mn, K, Na, Ni, Zn, Co, Cr, and Sb. SiO_2 was determined from solution A using spectrophotometer. The content of CO_2 in magnesite was calculated by molecular recalculation method assuming that the elements with which CO_2 combines are Mg, Ca, Fe and Mn. Calculation was also made for the mole percent of different carbonates that are possibly found as a solid solution. These carbonates are magnesite, calcite, siderite and rhodochrosite. Loss on ignition was determined for some of the samples and are in agreement with the calculated values of CO_2.

5.3.3 Results of chemical analysis

Analytical data for 27 samples are presented in the form of oxides (Table 3). Standards employed to determine magnesium are PCC-1 and DTS-1. These analyses

reveal a rather uniform composition for the magnesite. The alkali oxides are generally low. Al_2O_3 is almost below the detection limit for most of the samples except few samples. FeO is computed as a total iron (+2) oxide, slight variation is observed for the iron oxide. Those samples with yellowish brown or with reddish tints have a slightly higher iron oxide content. Manganese is rather low and in most of the samples it is below the detection limit. Some variations in silica content of the analyzed samples is observed. This matches with the field observation of silica in the form of quartz and/or chalcedony. If there is visible quartz, the silica content will be higher. These relatively higher silica bearing samples usually represent contact zone where silicification is at a maximum. Magnesium content is generaly of economic grade, that is good quality magnesite. When the content of magnesium is lower, it means there are impurities such as silica and lime. Some of the vein materials have higher than normal calcium content.

Silica (SiO_2) content of the analyzed magnesites ranges from 0.59-7.05 weight percent and the average SiO_2 value is computed to be 2.38 with standard deviation and variance of 1.46 and 2.06, respectively. The silica has not such a regular trend of variation for different veins and stockworks. Variation may exist within one body of mineralization. It depends on the quality of the sample

analyzed. In most cases, samples taken from contact zones have a higher silica content.

CaO content of the analyzed magnesites ranges from 0.27-11.5 weight percent and the average amounts to 0.88%. The calcium oxide analyses have a variance of 0.35 and standard deviation of 0.61. This statistical value does not include the CaO values of two samples, M-8 and M-12. These two samples are taken from veins filling fault planes in Çakmak stockwork deposit. They have higher than normal value of CaO. M-8 has 9.83% CaO, which lowers the quality of magnesite. There is little market for magnesite containing more than 4% CaO (Bodenlos, and Thayer 1973). However, most of the analyzed samples are of economic grade. Samples from Çakmak stockwork deposit show a slightly higher CaO content than other vein type deposits. Generally, samples from the serpentinite where host rocks are highly altered to serpentine - carbonate rocks have higher CaO than vein type deposits outside the sheared serpentinite.

FeO analysis is reported as total iron. The FeO content in analyzed samples ranges from 0.3-6.05%. The mean of the analyses is 0.44 with standard deviation and variance of 1.17 and 1.32, respectively. No definite trend of variation is observed. Most of the samples are consistent in FeO value. Very small number of samples, M-6, M-10, and M-14, have values greater than 1%. This might represent iron from enclaves of rock fragments

contained in the magnesite ore of low grade type or most likely iron as siderite.

MgO content ranges from 35.83 - 46.79% with the mean value of 44.46 and standard deviation and variance of 2.68 and 6.95, respectively. As was mentioned earlier pure magnesite contains 47.8% of MgO. Most of the samples have economical MgO content. The mode of the analyses is 45% MgO indicating low level of impurity admixtures. However, few samples, M-12, M-8, M-6, M-13, M-14 and M-23 have MgO value less than the statistical mean value (44.46). This is due to higher CaO, FeO or silica contents. The relationship between MgO with silica, CaO and FeO is reciprocal. This situation is evident if we compare MgO and CaO values of M-24 (first grade ore) with that of M-8 (low grade ore). Both of these samples were taken from the same ore body, Çakmak stockwork deposit, but the former sample is taken from the main ore body whereas the later sample is that of low grade vein along a fault plane..

MnO ranges from 0.0 - 0.13% and has the mean value of 0.04 with standard deviation and variance of 0.04 and 0.001, respectively. Most of the samples show a value which is below the detection limit of 0.04%..

Alkalies (Na_2O and K_2O) and Al_2O_3 are very low in amount and some of the samples are below the detection limit (0.001%). The low level of total alkalies and Al_2O_3

content in ultramafic rocks of the study area are reflected by exceedingly small amounts of these oxides in magnesites, derived from ultramafic rocks.

NiO and Cr_2O_3 are common oxides of the country rocks, nevertheless, Cr_2O_3 is below the detection limit (not detected at all) for all the magnesite samples. However, the magnesites to some extent contain NiO; an average of which is 0.028% with variance of .0008 and standard deviation of 0.03. The absence of Cr_2O_3 might be due to resistance of chromite to decomposition, because, sometimes it is possible to see grains of shinning chromite in magnesite.

Analyses was also made for Zn and Sb, the later, Sb, is below the detection limit (not detected at all) whereas exceedingly small amount of Zn is detected, but most of the samples are still below the detection limit and are not included in Table 3.

Assuming the calcite group minerals as a solid solution forming series the MgO, CaO, FeO and MnO of magnesite analyses are converted to their respective carbonates, namely, magnesite ($MgCO_3$), calcite ($CaCO_3$), siderite ($FeCO_3$) and rhodochrosite ($MnCO_3$). The analysed magnesites consist of 80.79 to 99.49 mole percent of $MgCO_3$, 0.49 to 18.62 mole percent of $CaCO_3$ and traces of $FeCO_3$ and $MnCO_3$ (see table 3).

Table 3. Chemical composition of Harmancik magnesites

wt %	M-1	M-2	M-3	M-4	M-5	M-6
SiO_2	2.67	2.42	1.67	3.34	2.5	1.81
Al_2O_3	--	--	--	.22	--	1.56
FeO^T	.11	.30	.13	.14	.09	6.05
MgO	45.25	45.25	45.52	45.25	44.77	40.83
CaO	.32	1.46	1.18	.61	.50	2.14
Na_2O	.02	--	--	.04	.05	.04
K_2O	.00	--	--	.03	.11	.03
MnO	--	--	--	--	--	.06
NiO	.01	.02	.007	.00	.02	.118
Cr_2O_3	--	--	--	--	--	.30
CO_2	49.74	50.75	50.72	49.96	49.35	47.40
Total	98.13	100.2	99.26	99.60	97.39	100.03
Mole %						
$MgCO_3$	99.35	97.39	98.00	98.89	99.06	94.05
$CaCO_3$	.50	2.26	1.83	.94	.81	3.54
$FeCO_3$	.15	.35	.17	.17	.10	2.34
$MnCO_3$	--	--	--	--	.03	.07

FeO^T total iron oxide
CO_2 calculated

Table 3 Cont'd

wt %	M-7	M-8	M-9	M-10	M-11	M-12
SiO_2	.59	2.00	1.78	1.12	.57	3.01
Al_2O_3	--	3.37	--	.08	--	.08
FeO^T	.06	.19	.07	1.31	.1	.43
MgO	46.76	36.46	45.22	45.60	46.29	35.83
CaO	.34	9.38	1.14	.77	.96	11.50
Na_2O	.001	--	--	--	.003	.02
K_2O	--	--	--	.01	--	.02
MnO	.13	.08	--	.01	.004	.03
NiO	.005	.09	.01	.02	.005	.07
Cr_2O_3	--	--	--	--	--	--
CO_2	51.44	47.73	50.835	1.21	51.36	48.42
Total	99.32	99.75	99.32	100.1	99.29	99.39
Mole %						
$MgCO_3$	99.26	83.40	97.14	97.21	98.42	80.79
$CaCO_3$	.50	16.15	2.24	1.19	1.46	18.62
$FeCO_3$	.07	.33	.62	1.56	.11	.53
$MnCO_3$	.17	.12	--	.04	.01	.06

Table 3 Cont'd

wt %	M-13	M-14	M-15	M-16	M-18	M-18a
SiO_2	7.05	2.02	1.58	1.04	3.24	1.52
Al_2O_3	--	--	--	--	--	--
FeO^T	.11	1.54	.07	.13	.06	.1
MgO	43.66	43.81	46.49	46.36	45.58	44.29
CaO	.34	2.34	.27	1.04	.41	.32
Na_2O	--	--	.01	.03	.001	.001
K_2O	.02	--	.00	.14	.03	--
MnO	.006	--	.02	--	.01	--
NiO	.01	.007	--	.01	.01	.014
Cr_2O_3	--	--	--	--	--	--
CO_2	48.01	50.61	51.02	51.52	50.15	48.67
Total	99.21	100.32	99.46	100.30	99.48	94.87
Mole %						
$MgCO_3$	99.29	94.52	99.49	98.25	99.24	99.36
$CaCO_3$	.56	3.61	.41	1.59	.63	.51
$FeCO_3$	.14	1.87	.07	.16	.07	.13
$MnCO_3$	.01	--	.03	--	.06	--

Table 3. Cont'd

wt%	M-19	M-20	M-21	M-22	M-23	M-24
SiO_2	3.29	3.35	3.41	2.37	5.84	.74
Al_2O_3	--	--	--	--	--	--
FeO^T	.03	.14	.04	.16	.17	.17
MgO	44.77	44.58	45.60	45.98	43.86	46.79
CaO	.55	.63	.32	.59	.59	.59
Na_2O	.02	.04	.01	.01	.03	.001
K_2O	.01	.02	--	.01	.77	--
MnO	.02	--	--	--	--	.01
NiO	.003	.009	.02	.01	.02	.021
Cr_2O_3	--	--	--	--	--	--
CO_2	49.35	49.27	50.06	50.82	48.45	51.56
Total	98.04	98.03	99.43	99.96	99.73	99.89
Mole %						
$MgCO_3$	99.06	98.80	99.46	98.91	98.84	99.08
$CaCO_3$	.87	1.01	.49	.90	.94	.89
$FeCO_3$	.04	.19	.05	.19	.22	.02
$MnCO_3$	.03	--	--	--	--	.01

Table 3. Cont'd

wt%	M-25	M-26	M-27
SiO_2	1.55	2.50	1.37
Al_2O_3	--	.34	--
FeO^T	.06	.16	.16
MgO	45.29	44.53	45.95
CaO	1.98	1.52	.99
Na_2O	--	.03	.01
K_2O	--	.02	--
MnO	--	.021	--
NiO	.01	.03	.034
Cr_2O_3	--	--	--
CO_2	51.04	49.92	51.04
Total	99.53	99.07	99.55
Mole %			
$MgCO_3$	96.88	97.39	98.29
$CaCO_3$	3.03	2.38	1.50
$FeCO_3$	.09	.2	.21
$MnCO_3$	--	.03	--

5.4 Genesis

5.4.1 The System MgO-SiO2-H2O-CO2

Rocks consisting dominantly of two or more components of the system MgO-SiO2-H2O-CO2 include dunite, serpentinite, talc, and magnesite deposits. Magnesite generally occurs in association with quartz, talc, serpentine, anthophyllite, or enstatite.

In the system MgO - SiO2 - H2O - CO2, Johannes (1969) considered all equilibrium reactions that occur at higher pressures and temperatures and presented experimental determinations of the dependence of the equilibrium temperature upon pressure and composition of the fluid phase for the following reactions:

$$\underset{\text{forsterite}}{2Mg_2[SiO_4]} + 2H_2O + CO_2 = \underset{\text{serpentine}}{Mg_3[(OH)_4 \mid Si_2O_5]} + \underset{\text{magnesite}}{MgCO_3} \quad (1)$$

$$\underset{\text{forsterite}}{4Mg_2[SiO_4]} + H_2O + 5CO_2 = \underset{\text{talc}}{Mg_3[(OH)_2 \mid Si_4O_{10}]} + \underset{\text{magnesite}}{5MgCO_3} \quad (2)$$

$$\underset{\text{serpentine}}{2Mg[(OH)_4 \mid Si_4O_{10}]} + 3CO_2 = \underset{\text{talc}}{Mg_3[(OH)_2|Si_4O_{10}]} + \underset{\text{magnesite}}{3MgCO_3} + 3H_2O \quad (3)$$

$$\underset{\text{talc}}{Mg_3[(OH)_2 \mid Si_4O_{10}]} + 3CO_2 = 4SiO_2 + 3MgCO_3 + H_2O \quad (4)$$

$$\underset{\text{serpentine}}{Mg_3[(OH)_4 \mid Si_2O_5]} + 3CO_2 = 2SiO_2 + 3MgCO_3 + 2H_2O \quad (5)$$

The reaction equilibrium is determined by two of the following three parameters: pressure, temperature and the composition of the fluid phase (expressed as mole percent or as mole fraction CO2, X_{CO_2} = mole CO2/(moles

CO_2 + moles H_2O). For the procedure on how the experiment was carried out the reader is referred to Johannes (1969).

Forsterite reacts with a fluid phase that is free from or contains only very little CO_2 to serpentine and brucite according to the equation (see Figure 39).

2 forsterite + $3H_2O$ = serpentine + brucite[$Mg(OH)_2$] (6)

Brucite is stable only at very low CO_2 contents of the fluid phase. At higher CO_2 content of the fluid phase reaction (6) is replaced by the reaction (1) (see Figure 39).

The equilibrium temperature of this reaction rises (at P_f = constant) with increasing CO_2 content of the fluid phase. Figure 39 shows that the equilibrium temperature must increase from about 380°C at about 0.5 mole percent CO_2 to 490°C at 6 mole percent CO_2 at P_f = 2000 bars.

Above 490°c at P_f = 2000 bars reaction (1) is replaced by the reaction (2).

The equilibrium curve for reaction (3) separates the stability field of the assemblage "serpentine + magnesite" from that of "Talc + magnesite". Serpentine can coexist only with a CO_2-poor fluid phase. Even 1 to 3 mole percent CO_2 at P_f = 4kbars and 400°to 500°C is enough to cause serpentine to react to talc and

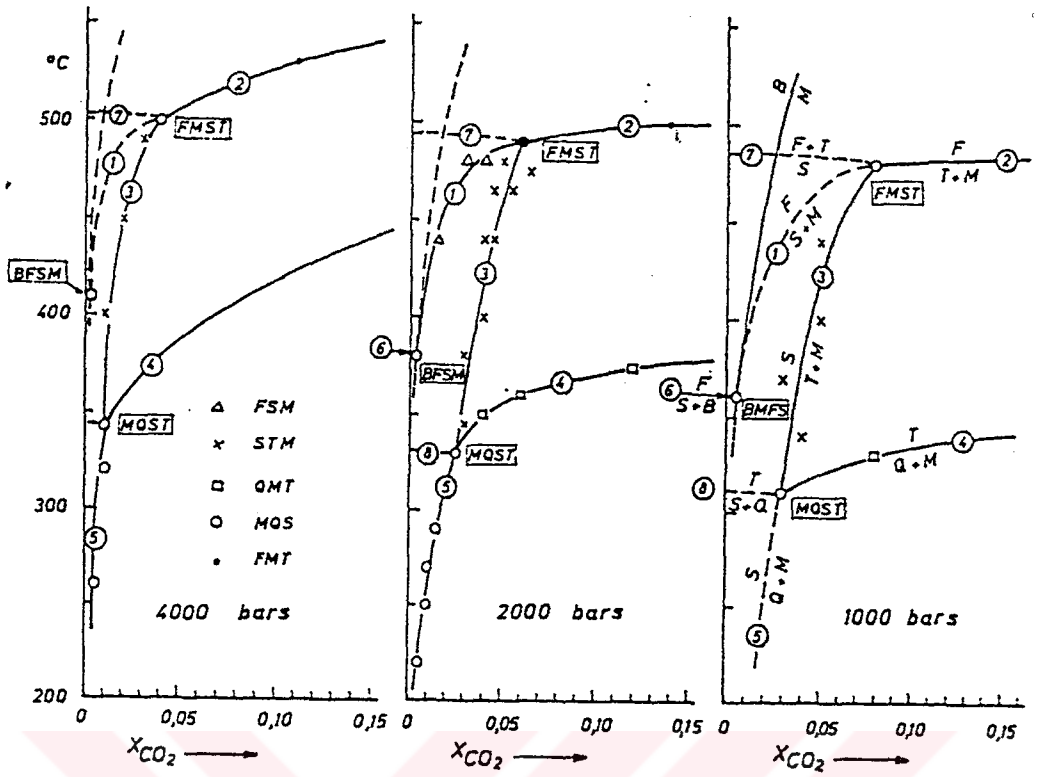

Figure 39. Isobaric equilibrium curves occurring at low CO2-contents of the fluid at Pf = 1000, 2000, and 4000 bars. Abbreviations: B: Brucite; F: forsterite; M: magnesite; Q: quartz; S: serpentine; T: talc.
(After Johannes, 1969)

magnesite. The presence of serpentine always indicates a low CO2 content of the formerly coexisting fluid phase.

Figure 39 shows that equilibrium curve (7) runs as a fourth curve from the indicated intersection point in addition to curves (1), (2) and (3) already discussed. This curve corresponds to the reaction

$$5\ MgSi_2O_5(OH)_4 = 6\ Mg_2SiO_4 + Mg_3Si_4O_{10}(OH)_2 + 9H_2O \qquad (7)$$

The equilibrium temperature of this reaction at P_{H_2O} = 2000 bars is 500°C (Bowen and Tuttle, 1949).

With a greater amount of CO2 in the fluid phase,

talc becomes unstable and reacts with CO_2 by the reaction (4).

The equilibrium temperature increases with increasing total pressure as well as with increasing CO_2 content of the fluid phase. Talc can be formed only as long as H_2O is still present in the fluid phase. At high CO_2 values, curve (4) is replaced by the rections involving anthophyllite or enstatite.

The position of equilibrium curves (3) and (4) in the T-Xco_2 diagram (see Figure 39) indicate that at low CO_2 contents of the fluid phase these curves intersect. The minerals quartz, magnesite , serpentine, and talc coexist at this isobaric invariant intersection point. Two further curves originate at the intersection of curves (3) and (4), for reactions (5) and (8):

serpentine + 2 quartz = talc and $1H_2O$ (8)

The lowest temperature at which talc can still be stable is, for example, almost 300°C indicating that talc is a metamorphic mineral in the system $MgO-SiO_2-H_2O-CO_2$.

Formation of magnesite along with quartz, chalcedony, opal, or flint from serpentine + CO_2 can be observed in rocks of ultrabasic composition according to the reaction (5). The position of equilibrium curve (5) in Figure 39 shows that even very low CO_2- values of the fluid phase can lead to formation of magnesite in serpentinites.

Equilibrium curves (13) and (14) (Figure 40) correspond to the following reactions

$$8\ \text{forsterite} + H_2O + 9CO_2 = \underset{\text{anthophyllite}}{Mg_7[(OH)_2/Si_8O_{22}]} + MgCO_3 \quad (13)$$

$$\text{anthophyllite} + H_2O + CO_2 = \text{talc} + \text{magnesite} \quad (14)$$

Equilibrium curves (15) and (16) (Figure 40.) result from the intersection point of curve (14) with (4). The corresponding reactions are:

$$1\ \text{anthophyllite} + 7CO_2 = 8SiO_2 + 7MgCO_3 + H_2O \quad (15)$$

$$4\ Mg_2[Si_2O_6] + H_2O + CO_2 = \text{anthophyllite} + \text{magnesite} \quad (16)$$

The intersection of curve (10) with (13) and of

$$(9\ \text{enstatite} + 2H_2O = 2\ \text{anthophyllite} + 2\ \text{forsterite}) \quad (10)$$

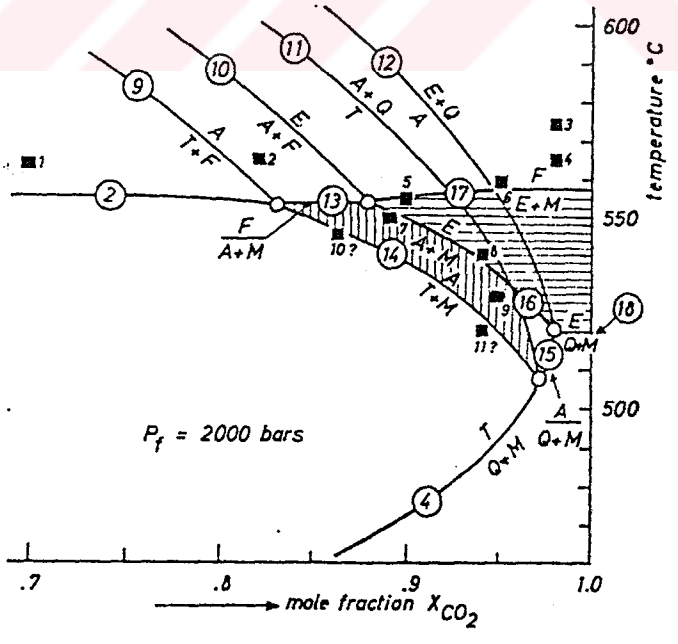

Figure 40. Phase relationships in the T-Xco_2-field in the region of high CO_2 - content of the fluid phase at Pf = 2000 bars. (After Johannes, 1969).

curve (15) with (16) produces equilibrium curves (17) and (18) corresponding to the equations

2 forsterite + $2CO_2$ = enstatite + 2 magnesite. (17)

'enstatite + $2CO_2$ = $2SiO_2$ + 2 magnesite (18).

According to Greenwood (1967) the stability fields of the assemblages anthophyllite + magnesite and enstatite + magnesite are limited to extremely low H_2O contents of the fluid phase.

5.4.2 Discussion

Magnesite occurs mainly in four types of deposits: as crystalline masses replacing dolomite, as impure crystalline masses replacing ultramafic rocks, as cryptocrystalline masses in ultramafic rocks, and as sedimentary beds and lenses (Bodenlos and Thayer 1973). Genetic models of the formation of cryptocrystalline magnesites include supergene and hypogene/hydrothermal variants. All models acknowledge, however, that the source of the Mg are the ultramafic host rocks of the deposits (Pohl, 1990).

Supergene models propose surficial disintegration and leaching of ultramafics within weathering profiles by rain water and/ or soil solutions, which seep into fractures of the underlying rocks where magnesite or a hydrous precursor is precipitated (Pohl, 1990).

Hypogene model proposes aqueous waters charged with CO_2 from a source at depth affect the ultramafic

country rock taking magnesium and silica in solution and carry them upward to a zone where supersaturation due to decrease in the partial pressure of the carbon dioxide causes deposition of magnesite (Pohl, 1990). Opal, chalcedony, and hydrous magnesium silicates followed the deposition of magnesite (Dabitzias, 1980).

The other hypothesis for the formation of cryptocrystalline ultramafic related magnesite is metasomatic in situ replacement of the ultramafic rocks. According to this hypothesis, descending meteoric waters or ascending CO_2-bearing hydrothermal solutions alter the host rocks and the resultant magnesite occupies the space of the original rock (Pohl, 1990). In Harmancik, most of vein-type magnesite deposits have sharp contacts with the host ultramafic rock which contradicts the metasomatic replacement. Furthermore, the angular fragments of serpentinite in stockwork deposit and the little or the absence of chromite in the veins all make this hypothesis of formation an unlikely possibility for Harmancik magnesite deposits.

The main evidence brought forward in support of a supergene origin of the mineralizing solutions (Dabitzias,1980) is the restricted depth of the deposits, the nodular structure of some magnesite, the purity of the magnesite, and the association of central European magnesite with weathered surfaces. However, Pohl (1990) presented observations that appear to contradict the

supergene model:

-The large open spaces needed, if Mg is introduced from the weathering zone into the later veins.

-The permeability problem, if magnesitization of the ultramafic rock in situ by descending CO_2 solution is considered. This results from the volume balance of the following (schematic) carbonation reaction:

$$\underset{100\ cm^3}{Mg_2SiO_4} + 2CO_2\ aq = \underset{130.7\ cm^3}{2MgCO_3} + \underset{52.7\ cm^3}{SiO_2\ aq}$$

Silica and part of the magnesite would have to be removed from the site of carbonation to allow for the volume balance

-supergene models often invoke close relations to lateritic weathering; which is not the case for most of ultramafic related deposits

-supergene models invoke downward transport of water, CO_2, and Mg with some Ca, while silica has to be removed.

According to Pohl (1990) ultramafic related magnesite deposits, such as Harmancik magnesite deposits, are modeled as a near surface epithermal-hydrothermal system (Figure 41).

Pohl's (1990) model proposes that aqueous solutions of moderate temperature and low salinity carrying CO_2 affect the ultramafic country rock by reactions of hydration and carbonation, which may

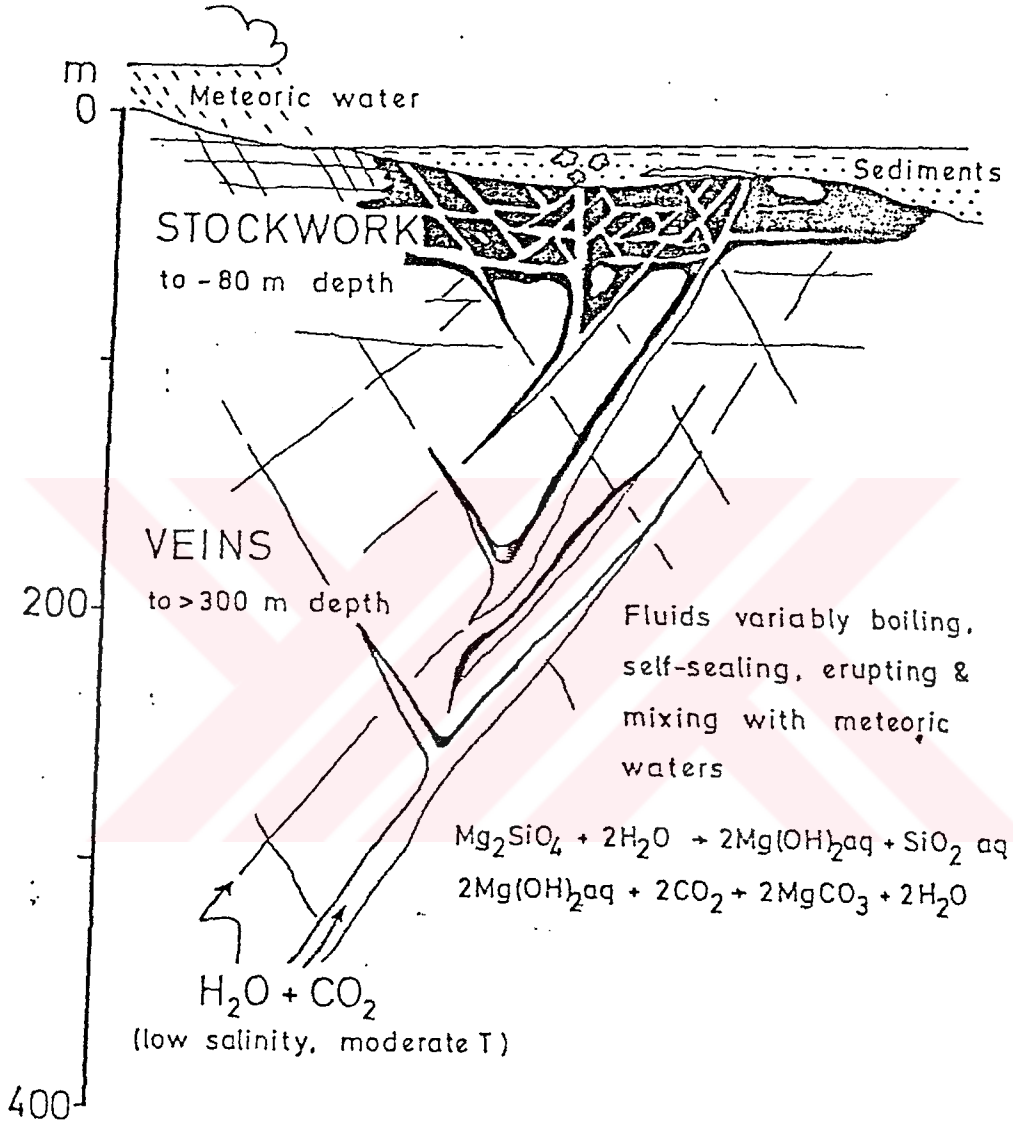

Figure 41 cryptocrystalline magnesite deposit modeled as a near surface epithermal system (After Pohl 1990).

schematically be written

$$Mg_2SiO_4 + 2H_2O = 2Mg(OH)_2\ aq + SiO_2\ aq$$

$$2Mg(OH)_2\ aq + 2CO_2 = 2MgCO_3 + 2H_2O$$

The fluids in the fractures are variously boiling, self sealing and erupting. Nearer to the surface, mixing with meteoric water may occur. Most of the iron and silica derived from decomposition of the country rocks is carried towards the surface, while magnesium carbonate or a hydrous carbonate precipitates nearly in situ as gel.

Pohl (1990) concludes that the near surface epithermal-hydrothermal model of the origin of cryptocrystalline magnesite deposits appear to be more probable than supergene formations. Pohl (1990) pointed out that the data is far from complete and recommended research to continue.

CHAPTER VI

CHROMITE DEPOSITS

6.1 Geological Description

Turkish ultramafics received attention with the first discovery of chromite in 1848 by Lawrence Smith at Harmancik (Tankut, 1977). The ultramafic rocks of the study area are hosts not only for magnesite deposits but also for chromite deposits. The chromite deposits in the region are of podiform - type which are characteristic of alpine peridotites. Podiform chromite deposits are lenticular concentrations of massive to disseminated chromite that occur in dunites and harzburgites of ophiolite complexes and are distinctly elongate (Dickey, 1975). They are typically surrounded by dunite halos beyond which the country rock is harzburgite or, less commonly, dunite (Dickey, 1975). Nodular texture is a critical feature that distinguishes podiform chromite deposits from all others, and particularly from stratiform deposits (Thayer, 1969). As pointed out by Thayer (1964) the podiform chromite deposits almost always have undergone some kind of metamorphic deformation and should be considered as metamorphic rocks.

Numerous pods of chromite were outlined in the

area mapped (see Appendix A.1). The areal extent and the depth of these pods were not possible to estimate. However, the trend as well as the continuity of the chromitite pods were outlined. There are numerous small galleries and trenches made for the purpose of mining the chromite deposits. Wherever the chromite pod is found the host rock is dunite. Almost all the chromites are found in the dunite; harzburgites are devoid of chromite pods. The contact that the chromitite forms with its host dunite is gradational. Olivine is the major gangue mineral in the chromitite body and its amount becomes higher near contact zones. The structure is rather massive and in the main ore body chromite is the major mineral. The close association of chromite and olivine indicate that these two minerals crystallize together in the early history of magmatic differentiation.

Chromitite concentrations are prominent near Çatal Tepe and Hazne Tepe. The chromitite lenses have a general NE trend steeply dipping about 60° towards NW. The serpentinite (alteration zone), which is outlined in the geological map (Appendix A.1), has very small number of chromitite pods. In the study area, where magnesite mineralization is intense chromite become less important and where the concentration of chromite pod is higher there is almost no magnesite. Nevertheless, near Kalempinar Tepe a close association of chromite body and magnesite vein was noted.

6.2 Mineralogy

Polished section studies indicate that the chromite deposits have rather simple mineralogy. No other ore minerals associates chromite.

Cataclastic texture characterizes the chromites (Figure 42) indicating the imposed deformational episode. The individual chromite grains are crushed and olivine or serpentine fill these cracks. In many cases the individual grains of chromite show a pull-apart texture related to their metamorphic deformation (Figure 43).

Nodular texture is by far the distinct feature of chromite of the study area (Figure 44). The nodules are the aggregates of chromite grains. Thayer (1969) suggests a process of very slow accumulation of chromite or associated minerals from the source material. Dickey (1975) suggests a process of snowballing and recrystallization of chromite crystals in a turbulent zone of magma segregation.

Thayer (1970) pointed out that the chromite composition conforms to the general formula AB_2X_4 which may be modified to $R^{+2}R^{+3}_2O_4$ or $RO.R_2O_3$. RO consists principally of MgO and FeO, but includes also MnO, NiO, and ZnO; R_2O_3 consists of Cr_2O_3, Al_2O_3, Fe_2O_3 and V_2O_3. The general formula of chromite is $(Fe^{+2}, Mg)(Cr, Al, Fe^{+3})_2O_4$, of which the end-members are chromite ($FeCr_2O_4$), hercynite ($FeAl_2O_4$), magnetite ($FeFe_2O_4$),

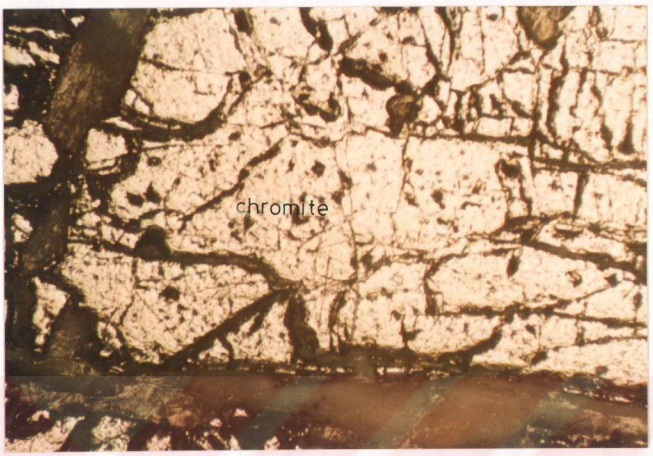

Figure 42. Photomicrograph of chromite showing cataclastic texture (sample no. C-2, crossed nicols x40)

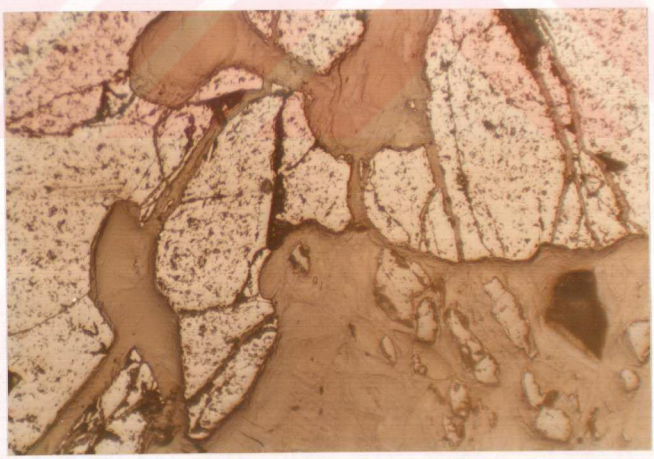

Figure 43. Photomicrograph of chromite showing pull-apart texture (sample no. C-1, crossed nicols x40).

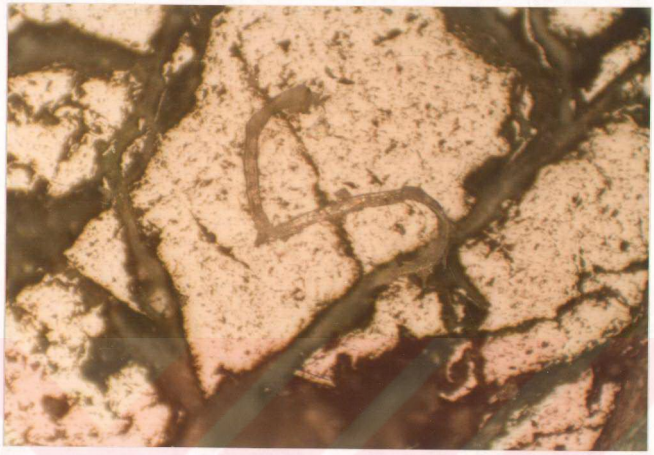

Figure 44. Photomicrograph of chromite showing nodular texture (sample no. C-6, crossed nicols).

picrochromite ($MgCr_2O_4$), spinel ($MgAl_2O_4$) and magnesioferrite ($MgFe^{+3}O_4$) (Irvine, 1965).

X-ray diffraction study of the chromites was made using JEOL JSDX 100S diffractometer with operating conditions of 40kv voltage 30mA current and Ni-filtered CuKα radiation. Powder samples were filled into a container with a hollow at the center (2 x 2 cm and 2 mm depth) and scanned from 2° to 60° 2θ at a rate of 1°/ minute. The XRD patterns of two samples were studied (C-5 and HC-1) out of which the diffraction pattern of only one sample (C-5) is presented here (Figure 45).

The X-ray diffraction data for the chromite is comparable to the ASTM (American Standard Testing and Material) standard chromite (card 3-0873) for the spacings (111), (022), (113) and (222). The (100) and (203) reflections at 2θ values of 24.2° and 34.1° indicate the presence of antigorite (serpentine) within the sample. Data obtained from diffraction pattern of Figure 45 are presented in Table 4. For various reflections d spacings are determined together with their intensity of reflection. Using these data the unit cell edge (a_o) of chromite (cubic system) are determined according to the relation (Hutchison, 1974) $a_o = d_{hkl} * SQR (h^2 + k^2 + l^2)$. Error in cell parameter is minimized by plotting the a_o value versus Nelson & Riley function in order to get the closest a_o value of chromite (Figure 46). The a_o value is determined to be $8.327 A^{\circ}$.

Based on the data of chemical analyses of chromite which indicates the presence of appreciable amount of MgO and Al_2O_3 in chromite it has been tried to determine the percentage composition of the end members chromite ($FeCr_2O_4$) and spinel ($MgAl_2O_4$). The method involves plotting the cell dimensions of pure chromite and pure spinel against the percentage of these end-members (Figure 51). By make use of the error free unit cell edge of the sample $a_o = 8.327$ the chromite end member is 76% whereas the spinel is 24%.

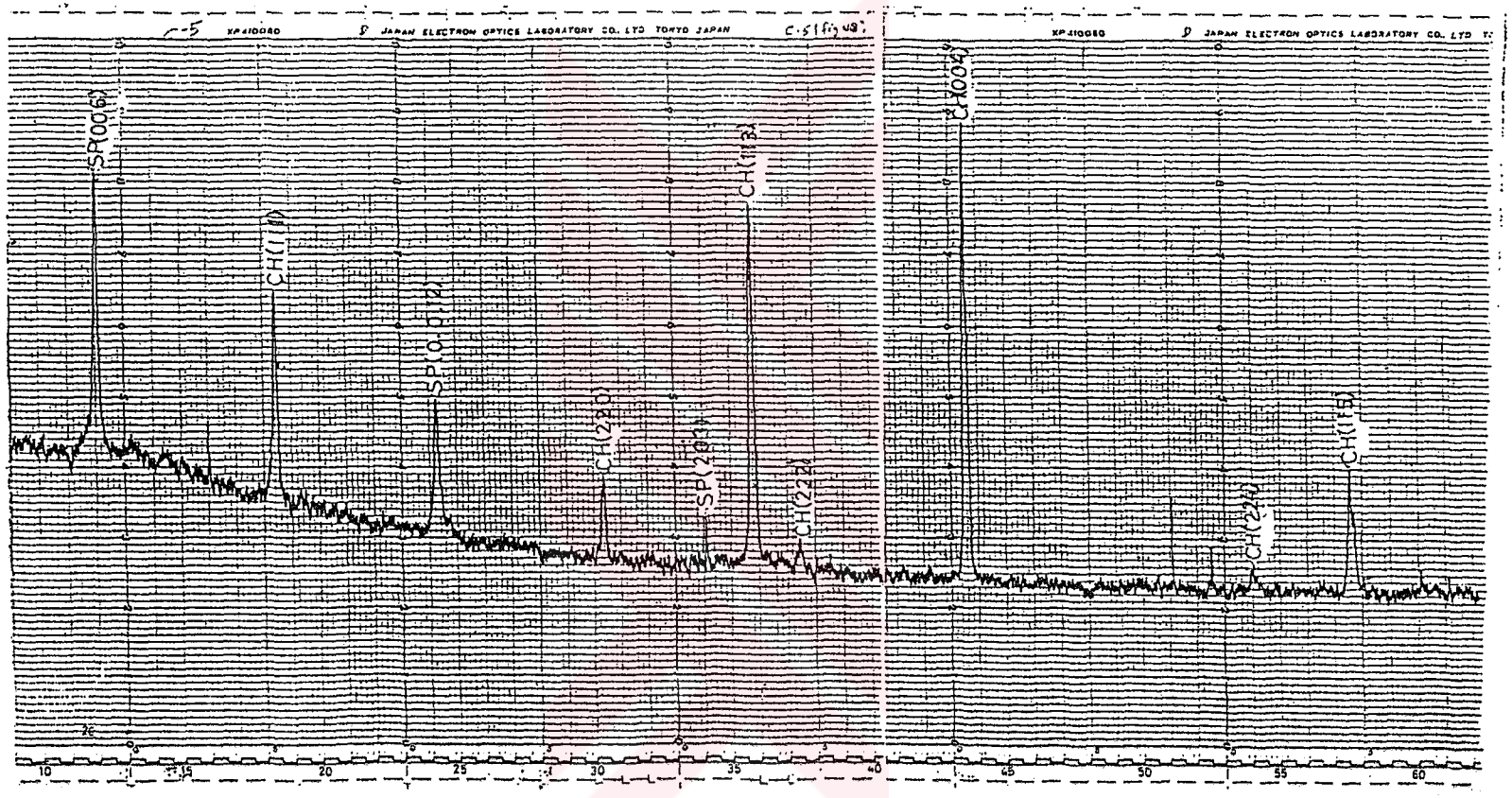

Figure 45 X-ray diffraction pattern of chromite (CH) containing serpentine (SP) (sample no. C-5)

Table 4. Data obtained from the diffraction pattern of chromite

, 2θ	d	I	hkl	ao	Nelson & Riley fun.
18.5	4.79	50	111	8.2965	3.0572
30.39	2.9411	60	022	8.3186	1.8071
35.80	2.5081	100	113	8.3184	1.4952
37.50	2.3982	10	222	8.3076	1.4184
43.50	2.0804	70	004	8.3216	1.1838
54.00	1.6980	40	224	8.3184	.8887
57.60	1.6000	90	115	8.3138	.8103

6.3 Geochemistry

Five chromite samples were analyzed for major and trace elements using AAS and spectrophotometer. H_2SO_4 + H_3PO_4 acid mixture were used to decompose chromites the procedure of which is shown in Appendix B.3. Elements determined by AAS are: Cr, Al, Fe, Mg, Ca, Na, Mn, Ni, and Zn. Silica was determined from solution A (Appendix B.2) by using spectrophotometer.

Table 5 presents the analyses of 5 chromite samples (C-2, C-5, C-6, C-8, and HC-1). Silicate impurity which is found in the ore is reflected as SiO_2. The oxides were recalculated on a SiO_2 free basis (Table 6). Recalculation involves subtraction of MgO and FeO based

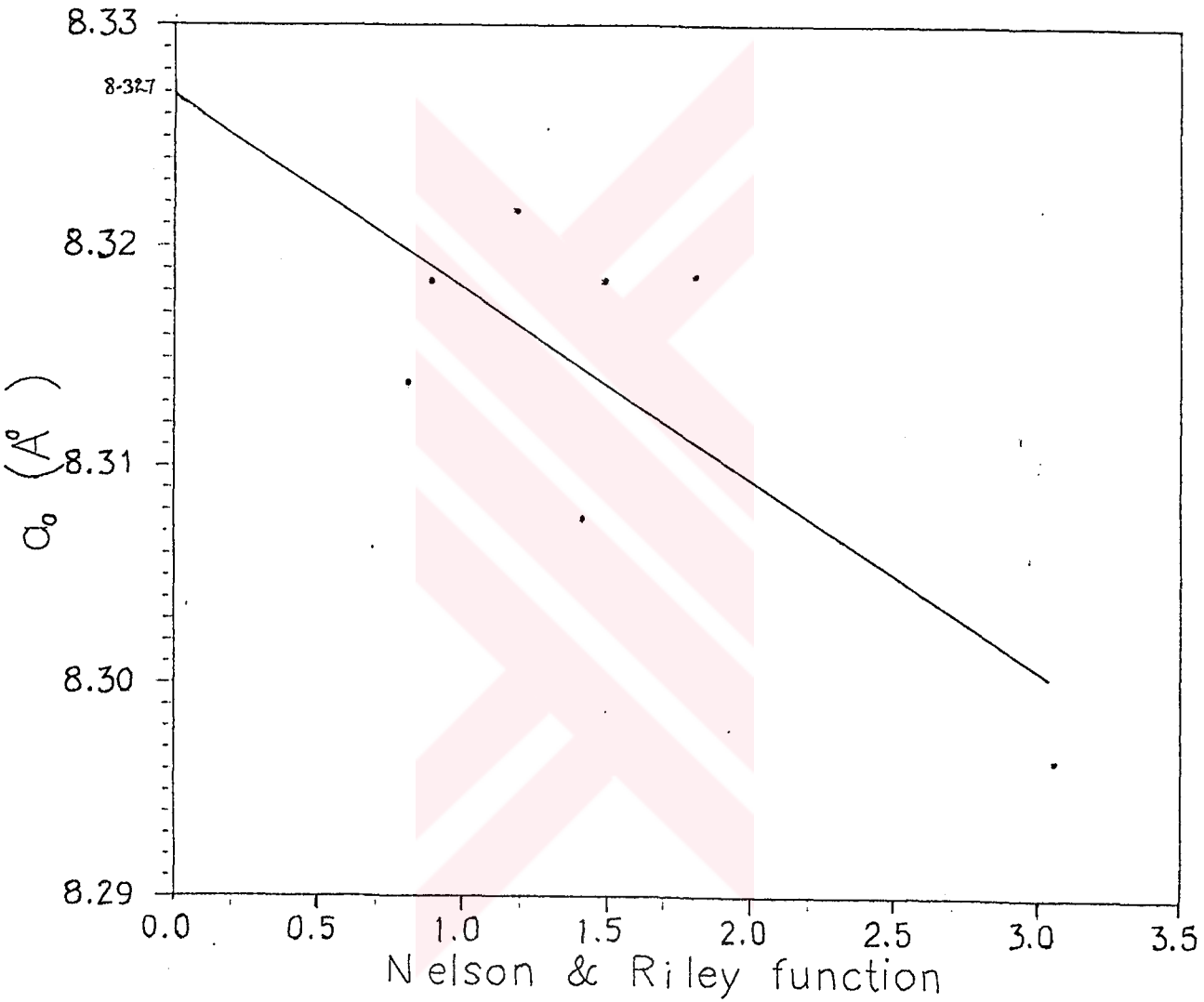

Figure 46 The binary plot of unit cell dimension versus Nelson & Riley function

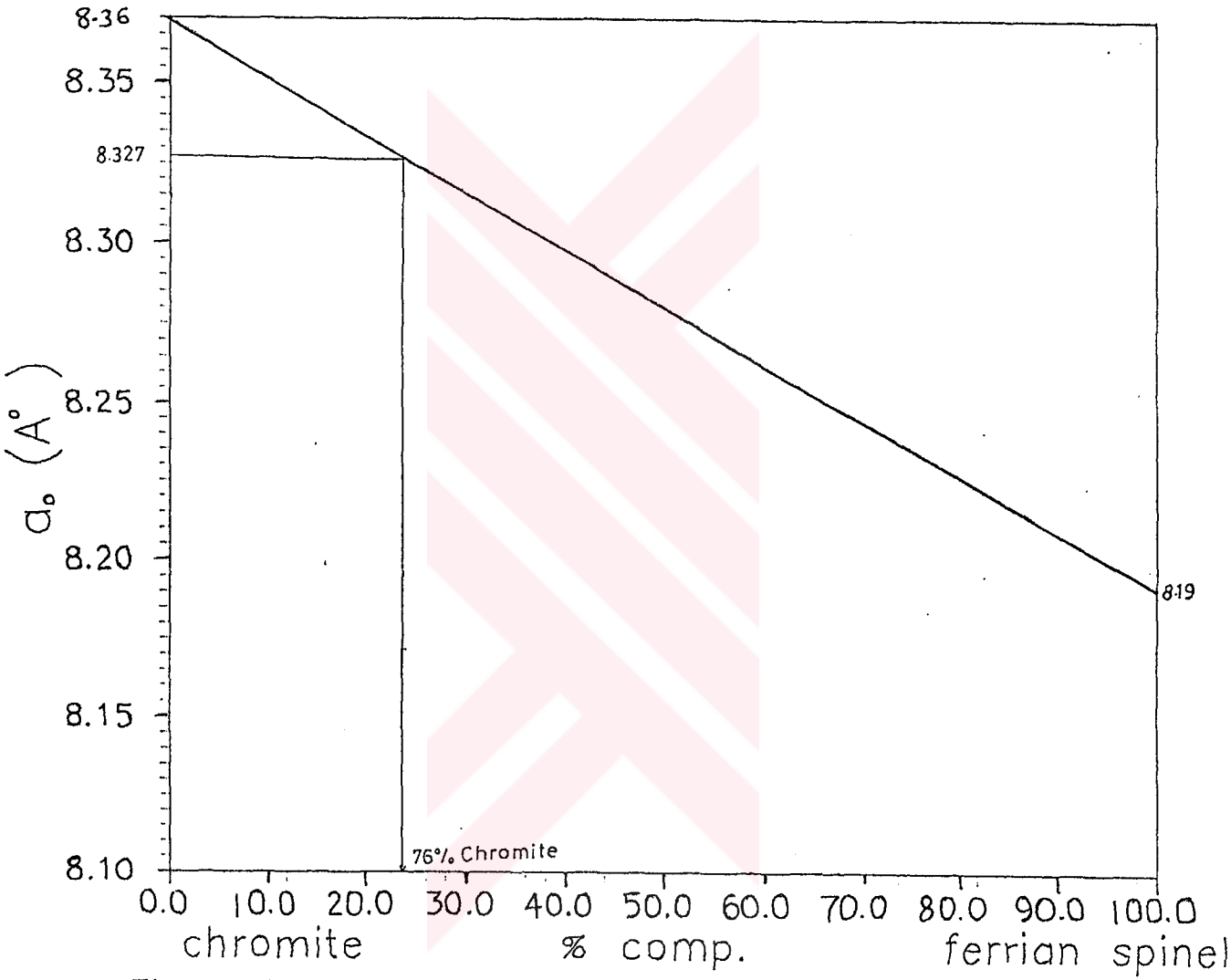

Figure 47 Plot of cell dimensions of pure chromite and spinel Versus the percentage composition of these end members (sample no. C-5)

on 91% Fo and 9% Fa (result obtained from XRD study) by making use of the procedure in Appendix C.1. The Cr_2O_3 content ranges from 45.12-50% and the Al_2O_3 content range from 14.03-15.62%. The trivalent and bivalent Fe were calculated from the total Fe assuming the stoichiometry of chromite as R_2O_3:RO being equal to 1 (Appendix C.2).

The plot of unit cell composition of chromites on a triangular diagram falls within aluminian chromites (Figure 48). The binary plot of Fe^{+2}/ Mg+ Fe^{+2} versus Cr/

Table 5. Chemical composition of the Harmancik chromites

wt %	C-2	C-5	C-6	C-8	HC-1
Cr_2O_3	48.32	47.56	49.52	45.12	50.26
Al_2O_3	15.38	15.62	14.81	14.03	14.45
MgO	17.26	19.24	18.47	20.08	18.02
FeO^T	12.21	10.85	11.17	13.81	12.25
SiO_2	5.32	5.48	5.28	4.24	3.98
CaO	.10	.11	.17	.15	.16
Na_2O	.56	.63	.49	1.64	.40
MnO	.07	.09	.06	--	.14
NiO	.29	.24	.28	.28	.12
ZnO	.13	.16	.14	.13	.22

Al + Cr and Fe^{+3}/ Cr + Al + Fe^{+3} falls within the field of podiform chromite deposits (Figure 49).

The structural formulae of chromites are calculated on the basis of 32 oxygen atoms as the unit cell contains 8 bivalent, and 16 trivalent cations and 32 oxygen. The structural formula of studied chromites are shown in Table 7.

Table 6 Correction of the Harmancik chromites after normative olivine and ferrous and ferric iron calculations

wt %	C-2	C-5	C-6	C-8	HC-1
Cr_2O_3	48.32	47.56	49.52	45.12	50.26
Al_2O_3	15.38	15.62	14.81	14.03	14.45
MgO	10.75	12.62	12.03	14.94	13.18
FeO^T	11.06	9.61	10.00	12.89	11.36
Fe_2O_3	4.09	5.46	4.92	10.96	4.75
FeO	7.52	4.70	5.74	3.41	7.25

Table 7. Recorrected chemical composition and structural elements of the Harmancik chromites

wt %	C-2	C-5	C-6	C-8	HC-1
Cr_2O_3	56.15	55.32	56.91	51.00	55.91
Al_2O_3	17.87	18.17	17.02	16.33	16.07
MgO	12.49	14.68	13.82	16.88	14.66
FeO^T	12.85	11.18	11.49	14.56	12.64
Fe_2O_3	4.75	6.35	5.65	12.40	5.28
FeO	8.74	5.47	6.60	3.85	8.07

structural elements

	C-2	C-5	C-6	C-8	HC-1
Cr	38.41	37.83	38.92	34.88	38.24
Al	9.45	9.61	9.00	8.64	8.50
Mg	7.53	8.85	8.33	8.33	8.84
Fe^{+3}	3.32	4.44	3.95	8.67	3.69
Fe^{+2}	6.79	4.25	5.13	2.99	6.27
Fe^T	9.98	8.69	8.93	11.31	9.83
Cr/Fe^T	3.85	4.35	4.35	3.08	3.89
Cr/(Cr+Al)	.80	.79	.81	.80	.82
$Cr/(Cr+Al+Fe^{+3})$	.75	.73	.75	.69	.76
$Al/(Cr+Al+Fe^{+3})$	.18	.19	.17	.16	.17
$Fe^{+3}/(Cr+Al+Fe^{+3})$	.06	.08	.07	.17	.07
Fe^{+2}/Mg	.90	.48	.62	.36	.71
$Fe^{+2}/(Mg+Fe^{+2})$	.47	.32	.38	.26	.41

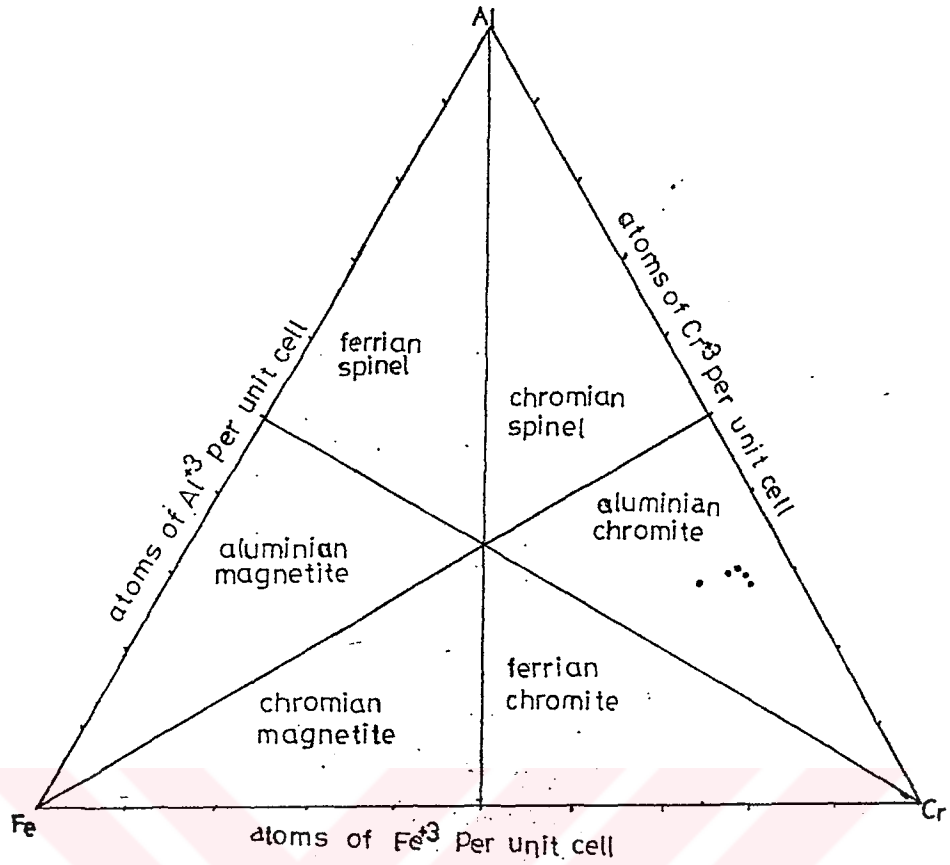

Figure 48. Chromite composition diagram (Stevense, 1944, in Tankut, 1977).

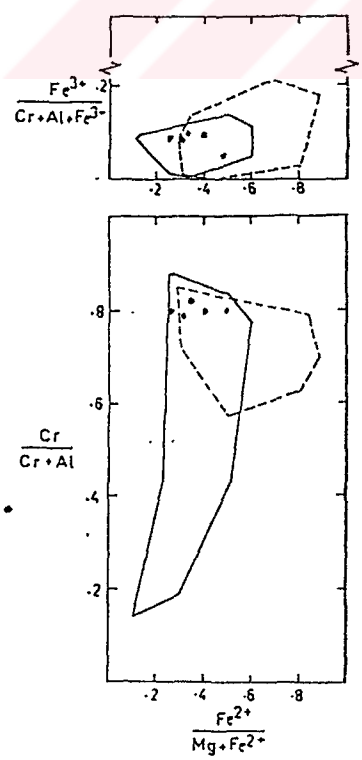

Figure 49. plot of Harmancik chromites on Cr/(Cr+Al) versus $Fe^{+2}/(Mg+Fe^{+2})$ and $Fe^{+3}/(Cr+Al+Fe^{+3})$ diagram
dashed line - stratiform
solid line - podiform

(After Greenbaum, 1977)

CHAPTER VII

CONCLUSIONS

The study area covering an area of 40 square kilometers was mapped at a scale of 1 : 25,000. The main rock units of the study area in descending age order are: Yanikkaş marble, Harmancik ultramafic complex, Gedikler granodiorite, and Çakmak Formation.

Rocks belonging to the Harmancik ultramafic complex are dunite, harzburgite, serpentinite and doleritic dikes. Economic mineral deposits contained within this complex are magnesite and chromite.

Petrographic studies indicated that harzburgite is more widespread than dunite. Both units are composed entirely of olivine, orthopyroxene (enstatite) and chromite as cumulus minerals. Rocks of the Harmancik ultramafic complex show the effects of tectonic deformation of various intensity. Most of the samples show cataclastic or crushed textures. Kink banding in orthopyroxene and strained olivines showing wavy extinction are evidences of tectonic activity and are metamorphic peridotites as Coleman (1977) suggested.

The rocks within the ultramafic complex are usually serpentinized to various degrees and it is rare

to find rocks that contain completely unaltered olivine and orthopyroxene. The intensity of serpentinization become higher along fault zones, shear zones, around intrusives and doleritic dikes. Mesh-texture is the typical feature of the serpentinized ultramafic rock. The slight variability in the chemical composition of the ultramafic rocks are attributed to the effect induced by serpentinization processes. Serpentinization involves addition of water and/or silica to convert dunite or harzburgite to serpentine bearing rock. Silica and water were added and magnesia was removed during serpentinization of the Harmancik ultramafic complex.

X-ray diffraction study of dunite and harzburgite indicates the composition of olivine to be 91% Fo and of orthopyroxene to be 93% En. These are in agreement with olivine and orthopyroxene compositional range reported by Tankut (1977) for Orhaneli ultramafic rocks.

Two forms of magnesite occurrence are recognized: stockwork type and vein type. The stockwork type deposits are restricted to the eastern part of the area in serpentinite and are characteristic of highly brecciated and serpentinized country rocks. Within this type of deposits, the crystalline as well as the yellow variety of magnesite is found.

The vein type deposits characteristically follow minor and major tectonic dislocations such as fault

planes and minor fractures. As a rule, the orientation of veins follow regional fracture patterns; footwalls of veins are often slickenside with thin serpentine or talc bands, while hanging walls may be breccias with a magnesite matrix grading into massive country rock. Wallrock alteration in the stockwork type deposits is pervasive, whereas veins have commonly only narrow alteration rims.

Johannes (1969) indicated that a fluid phase with very little CO_2 leads to the formation of serpentine and brucite from forsterite. The present investigation, however, confirms the absence of brucite in the mass of serpentinized ultramafic rock indicating that the fluid phase involved were rich in CO_2 than the amount needed to form the assemblage serpentine and brucite. In the Harmancik ultramafic complex the widespread occurrence of magnesite together with serpentinites and serpentinized country rocks clearly indicated that reaction (1) of Johannes (1969) is valid: at higher CO_2 content of the mineralizing fluid still serpentine forms together with magnesite from forsterite.

Talc forms either directly from forsterite or from further alteration of the already formed serpentine. In the study area, the amount of talc is very small, which is considered to point to the process of continuing serpentinization.

The current trend of thinking regarding the genesis of such magnesite deposits is modeled as a near surface epithermal - hydrothermal system and it states that the aqueous solutions of moderate temperature and low salinity carrying CO_2 affect the ultramafic rock by reaction of hydration and carbonation. The origine of magnesites of the study area is considered to be fracture fillings from mineralizing solution and is not metasomatic in situ replacement of ultramafic rock. Epithermal near surface model suggested by Pohl (1990) for the formation of Harmancik magnesites appears to be the most probable mechanism. This proposal is suported by the occurrence of magnesites only in sheared serpentinites and ultramafic rocks.

The other important economic mineral deposits of the Harmancik ultramafic complex are those of chromite. The chromite deposits are of podiform type which are characteristic of Alpine peridotites. The host rocks for almost all chromitites are dunites. Cataclastic and nodular textures are the typical features of the chromites. The chromites have the composition of aluminian chromites and are composed of 76.4% chromite ($FeCr_2O_4$) and 23.6% ferrian spinel ($(Fe^{+3},Mg)Al_2O_4$).

REFERENCES

————————, 1989. "Geological report for magnesite deposits in Emirköy - Çakmak areas-Harmancik", BATKO Geological Engineering consulting, Ankara, 30 p.

Bingöl, E., Delaloye, M. and Ataman, G., 1982, "Granitic intrusion in western Anatolia: a Contribution to the Geodynamic study of this area", Eclogae Geol. Helv., 75, 437 - 446.

Birch, R.E., and Wicken, O.M., 1985. "Magnesite and related minerals", cited in Industrial minerals and rocks [2nd ed.]: Amer. Inst. Mining, Metall., and petroleum Engineers, P. 521- 541.

Bodenlos, A.J. and Thayer, T.P., 1973. " Magnesian refractories", U.S. Geol. Serv. prof. paper 820, P. 379 - 384.

Borchert, H., and Uzkut, i., 1967. "Harmancik (Bursa ili) kuzeybatisindaki krom cevheri yataklari", M.T.A. Bulletin, no. 69, P. 49 - 63.

Bowen, N.L. and Tuttle, F., 1949. "The system MgO - SiO_2 - H_2O". Geol. Soc. Amer. Bull., 60, p. 439 - 460.

Coleman, R.G. (1977): Ophiolites, Springer - Verlag, Berlin, 229 p.

Dabitzias, S.G., 1980. "Petrology and genesis of the Vavdos cryptocrystalline magnesite deposits, Chalkidiki peninsula, Northern Greece". Economic Geol., 75, p. 1138 - 1151.

Dickey, J.S. Jr., 1975. " A hypothesis of origin for podiform chromite deposits", Geochim. Cosmochim. Acta, Vol.39, p.1061 - 1074.

Dubertret, L. and Kalafatçioglu, A., 1973: "Explanatory Text of the Geological Map of Turkey (1:500000 scale) Izmir Sheet", M.T.A. publication, Ankara, 115 p.+ map.

Göncüoglu, M.C., Özcan, A., Turhan, N. and Işik, A., 1992, "Stratigraphy of the Kütahya region" MTA - JMO, A Geotraverse across Tethyan Suture Zones in NW Anatolia, 3 - 11.

Greenbaum, D., 1977. "The chromiferous rocks of the Troodos ophiolite complex, Cyprus", Econ. Geol. v. 72, No.7, pp. 1175 - 1194.

Greenwood, H.J., 1967. "Mineral equilibrium in the system MgO - SiO_2 - H_2O - CO_2", cited in Research in Geochemistry, Abelson, P.H. (ed.): New York, London, Sydney, John Wiley and Sons, p. 542 - 567.

Himmelberg, G.R. and Coleman, R.G., 1968. "Chemistry of primary minerals and rocks from the Red - Mountain - Del Puerto ultramafic mass, California", U.S. Geolo. Survey professional paper 600-C, p. C18 - C26.

Hutchison, C., 1974. Laboratory Hand book of Petrographic Techniques, A Wiley - Interscience Publication, New York, 527 p.

Irvine, T.N., 1965."Chromian spinels as a petrogenetic indicator", part 1. Theory. Can. Jour. Earth Science, v.2, p. 648 - 672.

Johannes, W., 1969. " An experimental investigation of the system MgO - SiO2 - H2O - CO2", Amer. Jour. of Science, Vol. 267, p. 1083 - 1104.

Kalafatçioglu, A., 1962. "A note on the geology of the region between Tavşanli and Dagardi, and on the age of the serpentinites and limestones". M.T.A. Derg. no. 58, Ankara p. 38 - 46.

Lisenbee, A.L., 1971. "The Orhaneli ultramafic - gabbro thrust sheet and its surroundings", a progress report, cited in Geology and History of Turkey [Campbell, A.S., (ed.)], Petroleum Exploration Society of Libya, Tripoli, p. 349 - 368.

Möller, P., 1989. "Minor and trace elements in magnesite" , ccited in P. Möller (ed.), on the formation of magnesite, Borntraeger Monog. ser. Miner. Deposits, 28, p.173 - 196.

Okay, A.I., 1985, " Kuzeybati Anatolida Yer alan metamorfik Kuşahlar", Geolo. Soc. Turkey, Ketin

Simpozyumu, 83 - 92.

Pohl, W., 1990. "Genesis of magnesite deposits - models , and trends", Geologische Rundschau 79/2, p. 291 - 299.

Şengör, A.M.C., and Yilmaz, Y., 1981, "Tethyan Evolution of Turkey" A plate tectonic approach, Tectonophysics, 75, 181 - 241.

Tankut, A., 1977. "Petrology, geochemistry and mineralogy of Orhaneli ultramafic rocks and associated chromite deposits". Ph. D. thesis in Geological Engineering, Middle East Technical University, Ankara, 232 p.

Thayer, T.P., 1964. "Principal features and origin of podiform chromite deposits and some observations at the Guleman district, Turkey", Econ. Geol. 59. no. 8, p. 1497 - 1524.

Thayer, T.P., 1969. "Gravity differentiation and magmatic emplacement of podiform chromite deposits", Econ. Geol. Monog. 4, p. 132 - 146.

Thayer, T.P., 1970, "Chromite segregation as petrogenetic indicators", Geol. Soc. South Africa. Spec. Publ., 1, p. 380-390.

Zachmann, D.W. and Johannes, W., 1989. "Cryptocrystalline magnesite".-cited in P. Möller (ed.), on the formation of magnesite, Borntraeger Monog. Ser. Miner. Deposits. 28, 15 - 28.

APPENDICES

APPENDIX B

SOLUTION PREPARATION

B.1 Procedure for "Solution B" Preparation

(1) 0.2g powdered sample of -200 mesh size was weighed in a teflon beaker

(2) 15 ml of acid mixture (mixture of 400 ml HF, 165 ml H_2SO_4, and 40 ml HNO_3) is added to the sample in the teflon beaker and heated on the hot plate till complete evaporation and formation of a cake.

(3) 4 or 5 drops of acid mixture (a mixture of 100 ml $HClO_4$ and 100 ml HNO_3) is added to the cake in the teflon beaker and heated on the hot plate until complete evaporation.

(4) To the cake in the teflon beaker 5 ml HNO_3 and 15 ml distilled water are added and it is heated on the hot plate until the cake dissolves.

(5) After cooling the above solution it is transferred from teflon beaker to volumetric flask and diluted to 200 ml with water.

B.2 Procedure for "Solution A" Preparation

(1) 0.1g of sample and 3g (32 pellets) of NaOH are fused over a luminous flame in Ni -crucible.

(2) It is heated to dull redness for 5-8 minutes until fused.

(3) After cooling, the resulting cake is dissolved by water, until complete dissolution occurs.

(4) Contents of the crucible is poured into a beaker and 40 ml 3N H_2SO_4 is added.

(5) It is diluted to 1 lt with water.

B.3 Procedure for Chromite Decomposition

(1) 0.20 g cleaned chromite is weighed into glass beaker.

(2) 20 ml of $2H_2SO_4 + H_3PO_4$ is added

(3) It is boiled on a hot plate until to obtain clear solution.

(4) It is diluted to 200 ml and transfer into a plastic bottle.

APPENDIX C

CHEMICAL RECALCULATION

C.1 Rearrangement of MgO and FeO^T contents

1- $\frac{SiO_2\ \%}{\text{Mol. wt. of } SiO_2} : (SiO_2)$

$\frac{MgO\ \%}{\text{Mol. wt. of MgO}} : (MgO)$

$\frac{FeO^T\ \%}{\text{Mol. wt. of FeO}} : (FeO^T)$

2- $(SiO_2) \times 2\ (\%Fo) : MgO^X$

$(SiO_2) \times 2\ (\%Fa) : FeO^{TX}$

3- $MgO^! : (MgO) - MgO^X$

$MgO : MgO^! \times$ Mol. wt. of MgO

$FeO^{T^!} : (FeO^{TX})$

$FeO^T : FeO^{T^!} \times$ mol. wt. of FeO

C.2 Ferric and Ferrous Iron Calculations from Total Iron.

1- $\frac{Cr}{\text{At. wt. of Cr}} : (Cr)$

$\frac{Al}{\text{At. wt. of Al}} : (Al)$

$\frac{Fe^{T}}{\text{At. wt. of } Fe^{+2}} : (Fe)^{T}$

2- $R_2O_3 : RO : 1$

$(Cr) + (Al) + (Fe^{+3}) : 1$

$(Fe^{T}) : (Fe^{+3}) + (Fe^{+2})$

3- $(Fe^{+3}) : 1 - (Cr) - (Al)$

$(Fe^{+2}) : (Fe^{T}) - (Fe^{+3})$

4- $Fe^{+3} : (Fe^{+3}) \times \text{At .wt. of } Fe^{+3}$

$Fe^{+2} : (Fe^{+2}) \times \text{At. wt. of } Fe^{+2}$

5- $Fe_2O_3 : \frac{Fe^{+3}}{\text{Factor of } Fe^{+3}\ (0.6694)}$

$FeO : \frac{Fe^{+2}}{\text{Factor of } Fe^{+2}\ (0.7773)}$